Curvature-Mediated Interactions Between Membrane Proteins

K. S. Kim,* John Neu,# and George Oster§

*Department of Physics, Graduate Group in Theoretical Biophysics; #Department of Mathematics; and §Department of Molecular and Cellular Biology, University of California, Berkeley, California 94720 USA

ABSTRACT Membrane proteins can deform the lipid bilayer in which they are embedded. If the bilayer is treated as an elastic medium, then these deformations will generate elastic interactions between the proteins. The interaction between a single pair is repulsive. However, for three or more proteins, we show that there are nonpairwise forces whose magnitude is similar to the pairwise forces. When there are five or more proteins, we show that the nonpairwise forces permit the existence of stable protein aggregates, despite their pairwise repulsions.

GLOSSARY

$\mathbf{a}$ = Annulus surrounding a protein
a = Mean curvature bending modulus
b = Gaussian curvature bending modulus
a_1 = Dipole coefficient
$\mathbf{c}$ = Projection of $\mathbf{S}$ onto the base plane
$\mathbf{C}$ = Protein-bilayer contact curve on $\mathbf{S}$
E_m = Mean curvature energy
E_G = Gaussian curvature energy
f_C = Vertical force exerted along $\mathbf{C}$
$g(\mathbf{x})$ = Difference between two membrane configuration
h = Displacement field
$h_n \equiv \nabla h \cdot \hat{\mathbf{n}}$ = Normal derivative of h in the direction $\hat{\mathbf{n}}$
$\mathbf{J}$ = $\pi/2$ rotation matrix
l = Interprotein distance and lattice spacing
$\hat{\mathbf{n}}$ = Unit normal to curve $\mathbf{c}$
$\mathbf{P}$ = Arbitrary point on the membrane
$\mathbf{s}$ = Reference plane (projection of $\mathbf{S}$ onto base plane
$\partial\mathbf{s}$ = Boundary of reference plane
$\mathbf{S}$ = Membrane midsurface excluding proteins
$\partial\mathbf{S}$ = Boundary of membrane midsurface
$\mathbf{t}$ = Unit tangent to curve $\mathbf{c}$
$\hat{\mathbf{t}}$ = Unit tangent to the protein boundary curve
$\mathbf{w}$ = Rotation axis of a protein
$\mathbf{X}$ = Position vector on the bilayer manifold
$\mathbf{x}$ = Position vector in the base plane
z, ζ = Position vector in complex notation
η = Complex curvature scalar
γ = Contact angle between protein plane and membrane
$\kappa(\mathbf{x}) = \frac{1}{2}\nabla^2 h(\mathbf{x})$ = Mean curvature
$\boldsymbol{\kappa}_{1,2}$ = Principal curvature
$\boldsymbol{\kappa}$ = Extrinsic curvature tensor
$\det \boldsymbol{\kappa}$ = Gaussian curvature
$\boldsymbol{\omega}$ = $e^{2\pi i/5}$
$\phi(\mathbf{x})$ = Background curvature field
$\boldsymbol{\sigma} \subset \mathbf{s}$ = Subregion contained in $\mathbf{s}$ (also used to denote a region of a disk)
$\partial\boldsymbol{\sigma} = \partial\mathbf{s} + \mathbf{c}_r$ = Boundary of region $\boldsymbol{\sigma}$
$\boldsymbol{\tau}_c$ = Torque exerted on a protein with boundary curve $\mathbf{c}$
$\hat{\mathbf{1}}, \hat{\mathbf{2}}, \hat{\mathbf{3}}$ = Cartesian frame
$\mathbf{1_P}, \mathbf{2_P}, \mathbf{3_P}$ = Cartesian frame at point $\mathbf{P}$ on membrane
$\{\mathbf{1_P}, \mathbf{2_P}, \mathbf{3_P}\}$ = Cartesian unit vectors located at the point $\mathbf{P}$

INTRODUCTION

Proteins in biological membranes may constitute more than 50% of the surface area. Even proteins free to diffuse throughout the membrane frequently distribute themselves heterogeneously. To understand the distribution of proteins one must examine the interactions between proteins and between the proteins and the lipid bilayer. Recent studies have focused on interactions that are mediated by the elasticity of the membrane (Dan et al., 1993; Goulian et al., 1993; Mouritsen and Bloom, 1993). These interactions arise because an embedded protein creates a deformation field in the surrounding bilayer that influences neighboring proteins. The nature of this deformation field is dictated by the protein's elasticity and shape and by the membrane's elastic properties. In this paper, we examine the deformation field generated by proteins embedded in a membrane whose elastic energy is determined by its curvature. Previous work has revealed a long-range interaction between two proteins whose potential energy decreases with distance as $1/r^4$ (Goulian et al., 1993; Park and Lubensky, 1996). In the absence of thermal fluctuations ($T \equiv$ absolute temperature $= 0$), this $1/r^4$ interaction is repulsive. When $T > 0$, the interaction can be repulsive or attractive, depending on the bending rigidities of protein and membrane.

Received for publication 7 April 1998 and in final form 20 July 1998.

Address reprint requests to Dr. George Oster, Department of ESPN, University of California, 201 Wellman Hall, Berkeley, CA 94720-3112. Tel.: 510-642-5277; Fax: 510-642-5277; E-mail: goster@nature.berkeley.edu.

Dr. Kim's e-mail address is kkim@nature.berkeley.edu.

0006-3495/98/11/2274/18 $2.00

Here we examine the zero temperature limit more closely and demonstrate novel features that have been overlooked previously. Our results agree with prior studies of pairwise interactions; however, we show that the interaction between $N \geq 3$ proteins is not pairwise additive. Linear superposition of interactions no longer holds in this case. This has important and unforeseen consequences for how the proteins distribute themselves over the membrane. In particular, the pairwise repulsions may be opposed by nonpairwise forces, so that most of the proteins in a large aggregate do not contribute to the bilayer elastic energy. We will present simulations that demonstrate that these aggregates survive much longer than an ensemble of proteins subject to pairwise repulsions alone. Moreover, a finite number of proteins can self-assemble into stable equilibrium configurations despite the repulsive pairwise interactions. Furthermore, this equilibrium may be achieved for relatively small aggregates, with the time of equilibration decreasing with aggregate size. We will present some analytical results that shed light on the mechanisms leading to this counterintuitive result.

Protein clusters are the rule, not the exception, on most intracellular membranes. This is puzzling in some respects, because identical proteins would have identical charges, and so electrostatic forces would be unlikely to aid aggregation. As we show here, the nonpairwise nature of the curvature elastic forces mediated by the membrane is a likely candidate for the cohesive force that allows identical proteins to aggregate.

ELASTIC INTERACTIONS BETWEEN RIGID PROTEINS

We begin our analysis with the simplest case of rigid (inelastic) proteins embedded in a lipid bilayer; in a subsequent paper we will examine elastic proteins. The proteins bend the surrounding membrane, and this strain radiates outward, influencing neighboring proteins. We shall treat only small membrane deformations, and so we can model the membrane by its neutral surface, and the embedded proteins by a rigid surface embedded in the neutral surface. The geometry of the situation is shown in Fig. 1.

Denote by **S** the midsurface of the bilayer, and denote by **C** the curve representing the contact between the protein and midsurface **S**. We assume that the tangent planes of **S** along **C** are fixed once the protein position and orientation are set. **s** and **c** denote the projection of **S** and **C** onto the base plane. A rigid body motion of the protein induces corresponding rigid body motions of **C** and of the tangent planes of **S** along **C**. Points on the plane will be denoted by vectors $\mathbf{x} = x_1\mathbf{1} + x_2\mathbf{2}$, where $\{\mathbf{1}, \mathbf{2}\}$ are the horizontal Cartesian unit vectors (Fig. 1). In the limit of small deformations from a plane, it is convenient to describe the membrane neutral surface, **S**, by its elevation, $z = h(x)$, above the base plane. Thus points on **S** are specified by $\mathbf{X} = (\mathbf{x}, \mathbf{z}) = x_1\mathbf{1} + x_2\mathbf{2} + z\mathbf{3}$. Generally, we will denote quantities on the manifold, **S**, by uppercase symbols and those on the plane by lowercase symbols.

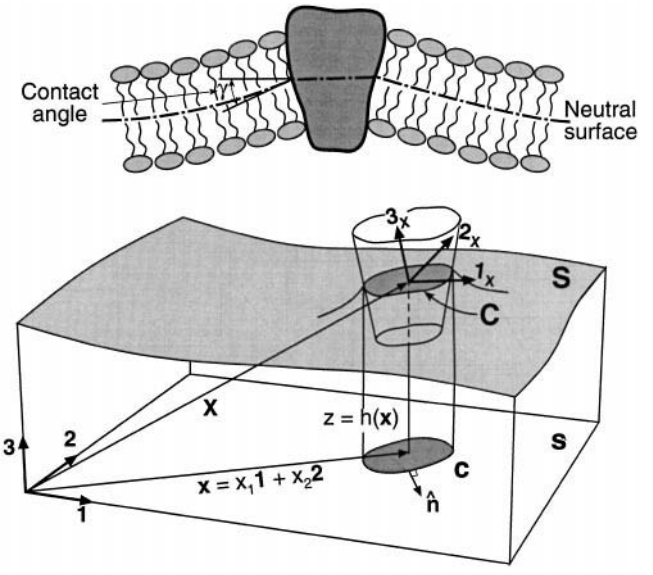

FIGURE 1 (*a*) A cross section of a bilayer in which a rigid protein is embedded. In the small deformation limit, the neutral surface coincides with the center surface. (*b*) The membrane surface **S** cuts the protein along the curve **C**. **s** and **c** denote the projections of **S** and **C** onto the base plane. $\hat{\mathbf{n}}$ denotes the outer normal of **c** in the base plane. The unit vectors in $\mathbf{R}^3 = \mathbf{s} \times \mathbf{R}^1$ are denoted by the boldface numbers $\{\mathbf{1}, \mathbf{2}, \mathbf{3}\}$.

Let $\kappa_1(\mathbf{X})$ and $\kappa_2(\mathbf{X})$ be the principal curvatures of **S**, which are functions of position on **S**. The energy per unit area of **S** is given by

$$E = 2a\left(\frac{\kappa_1 + \kappa_2}{2}\right)^2 + \frac{b}{2}\kappa_1\kappa_2 \tag{1}$$

where a and b are elastic constants. The inequalities $-4a < b < 0$ ensure positive definiteness. In Eq. 1, $(\kappa_1 + \kappa_2)/2$ is the mean curvature of **S**, and

$$E_{\mathrm{m}} \equiv 2a \int_{\mathrm{S}} \left(\frac{\kappa_1 + \kappa_2}{2}\right)^2 \mathrm{d}A \tag{2}$$

is the mean curvature energy of **S**. Here, $\mathrm{d}A$ is the area element on **S**. The quantity $\kappa_1\kappa_2$ is the Gaussian curvature of **S**, and the corresponding Gaussian energy of **S** is

$$E_{\mathrm{g}} \equiv \frac{b}{2} \int_{\mathrm{S}} \kappa_1\kappa_2 \, \mathrm{d}A \tag{3}$$

The model in Eqs. 1–3 is standard in the literature (Helfrich, 1973).

It is a well-known result from differential geometry that the integral of the Gaussian curvature over the surface **S** is related by Stokes' Theorem to a line integral over the boundary curve, $\partial\mathbf{S}$ (O'Neil, 1997). Here, the boundary curve includes the union of all of the protein boundary curves **C**, such as the one depicted in Fig. 1. This line

integral represents the contribution to Gaussian energy from all of these curves and is determined solely by the orientation of the planes tangent to **S** along them. As protein position and orientation change, the tangent planes along **C** undergo the same rigid body motion as the protein. The Gaussian energy line integral along **C** is a constant, independent of protein position and orientation, and so the Gaussian energy plays no role in the interaction between rigid proteins. Later, when we treat flexible proteins, the Gaussian energy will turn out to be important. Thus for rigid proteins, the elastic equilibria of the model are characterized by the minima of the mean curvature energy, which can be formulated as a variational problem. This problem has been well studied in the literature for both small and large deformations (Seifert et al., 1991).

In the small deformation limit with $|\nabla h| \ll 1$, the local mean curvature of **S** at a point $\mathbf{X} = \mathbf{x} + z\mathbf{3}$ is approximately $\frac{1}{2}\nabla^2 h(\mathbf{x})$. Therefore, the local mean curvature of **S** at **X** over a point $\mathbf{x} \in \mathbf{s}$ is approximated by

$$\kappa(\mathbf{x}) \equiv \tfrac{1}{2}\nabla^2 h(\mathbf{x}). \tag{4}$$

The mean curvature energy of **S** is an integral over its planar projection **s**:

$$E_m(\mathbf{X}) \approx \frac{a}{2}\int_s (\nabla^2 h(\mathbf{x}))^2 d\mathbf{x} = 2a\int_s \kappa^2 d\mathbf{x}. \tag{5}$$

In standard elastic plate theory, minimization of the energy (Eq. 5) leads to various boundary value problems (BVPs) for $h(\mathbf{x})$, depending on the physical constraints applied along the boundary $\partial\mathbf{s}$ (Timoshenko, 1987). In all of these BVP's, $h(\mathbf{x})$ satisfies the biharmonic equation

$$\nabla^4 h(\mathbf{x}) = 0, \quad \mathbf{x} \in \mathbf{s}. \tag{6}$$

Equation 6 expresses the balance of vertical forces on any infinitesimal patch of the bilayer (this is shown in Appendix A). Given an arbitrary solution, $h(\mathbf{x})$, of the biharmonic equation (Eq. 6), one can compute the net force and torque imposed by the bilayer on any one of the proteins embedded in it. For a true mechanical equilibrium, each rigid protein would have to be positioned and oriented so that all of the components of force and torque vanish. Here we will formulate a broader problem that contains the complete equilibria as a special case.

If the proteins embedded in the bilayer are not cylindrical prisms, they will induce curvature distortions in the surface **S**. For instance, a protein whose shape approximates an inverted, truncated cone will induce a dimple in the surrounding bilayer, as shown in Fig. 1. More generally, consider a finite collection of proteins in an unbounded bilayer. A given configuration of proteins specifies h and its normal derivative $h_n \equiv \nabla h \cdot \hat{\mathbf{n}}$ along all of the closed boundary curves of $\partial\mathbf{s}$ corresponding to projections of protein-bilayer contact curves onto the reference plane. If **s** were bounded instead of unbounded, specifying h and h_n along $\partial\mathbf{s}$ would be a proper set of boundary conditions for the biharmonic equation (e.g., clamped boundary conditions in plate theory), and a unique solution for h in **s** would be determined. The mean curvature energy E_m of **S** can then be computed from Eq. 5 as a function of protein configuration. However, if **s** is unbounded, the situation changes significantly. This is the case of interest in cells, for the dimensions of a cell are several orders of magnitude larger than those of the proteins and can be regarded as essentially infinite.

In this case, we seek biharmonic functions, $h(\mathbf{x})$, with boundary conditions for h and h_n along $\partial\mathbf{s}$ consistent with a given configuration of proteins. Because of the unboundedness of **s**, this class of solutions is quite large, and many of them do not have finite energy. However, if we require the elastic energy to be finite, this imposes certain force and torque balances on the proteins. The biharmonic equation (Eq. 6) for $h(\mathbf{x})$ implies that the mean curvature, $\kappa(\mathbf{x})$, is harmonic:

$$\nabla^2 \kappa(\mathbf{x}) = 0, \quad \mathbf{x} \in \mathbf{s}. \tag{7}$$

From Eq. 5 it is evident that the energy E_m is finite if κ is square integrable on **s**. From the requirements that κ be square integrable and harmonic in **s**, we show in Appendix A that the sum of vertical forces on all proteins induced by the bilayer vanishes, as does the sum of horizontal torques on all proteins.

The force and torque balances restrict the possible protein configurations, and one could now proceed to compute the (now finite) energy as a function of these restricted configurations. But the physically relevant configurations are subject to further restrictions: vertical force and horizontal torque balances apply to each protein individually. In Appendix B we show that the energy cost of violating individual force and torque balances is enormous. Certain consequences are clear: For an ensemble of proteins that are far apart compared to their radii, unbalanced vertical forces and horizontal torques on each protein will quickly equilibrate. These motions involve small vertical displacements of the proteins and small rotations about horizontal axes. After this rapid initial relaxation, the subsequent motions due to horizontal forces and vertical torques are much slower processes. The remaining horizontal forces and vertical torques can be computed from the energy projected onto the "slow manifold" of protein configurations with balanced vertical forces and horizontal torques on each protein. In fact, the energy computed within this constrained class of protein configurations contains the remaining horizontal forces and vertical torques within its variations.

To understand how force and torque balances constrain the protein configuration space, we can consider two configurations of the bilayer with the same embedded proteins. Both configurations have finite energy and are asymptotically flat, with unit normal **3** at infinity. Both configurations maintain a balance of vertical forces and horizontal torques on each protein. The only difference between the configurations is in the positions and orientations of the proteins.

We allow proteins of one configuration to be vertically translated with respect to those of the second and to be pivoted by small amounts about horizontal axes. Under these conditions, no horizontal pivoting is possible, and the only admissible vertical displacement is the same for all proteins. These results are shown in Appendix C. Thus restricting the allowable configurations to the above submanifold implies that the only surviving degrees of freedom are the positions and orientations of the closed curves, **c**, in the reference plane representing the protein-bilayer contacts. In summary, the proteins will adjust their relative positions (and their orientations if they are not circular) so as to satisfy the conditions of 1) finite energy, 2) asymptotic flatness, and 3) vertical and horizontal torque balance on each protein.

CIRCULAR PROTEIN SOLUTIONS AND THEIR ENERGETICS

Next we restrict our attention to a membrane system consisting of rigid proteins whose protein-membrane contact curve **C** is a unit circle, and the tangent planes of **S** along **C** have uniform contact angle, γ, as depicted in Fig. 1. Consider a single protein in an otherwise continuous unbounded bilayer. Cartesian axes $\hat{\mathbf{1}}, \hat{\mathbf{2}}, \hat{\mathbf{3}}$ are oriented so the origin is at the center of circle **C** and $\hat{\mathbf{1}}, \hat{\mathbf{2}}$ lie in the plane of the circle. Let (r, θ) be polar coordinates of the $\hat{\mathbf{1}}, \hat{\mathbf{2}}$ plane. The domain corresponding to the bilayer is $r > 1$. Boundary conditions along $r = 1$ are

$$h(r = 1, \theta) = 0 \tag{8}$$

$$h_r(r = 1, \theta) = -\gamma. \tag{9}$$

The biharmonic displacement field h in $r > 1$ satisfying these boundary conditions on $r = 1$ and asymptotic flatness at $r = \infty$ ($h_r \to 0$ as $r \to \infty$) is

$$h = -\gamma \ln r. \tag{10}$$

This single protein solution is not only biharmonic; it is harmonic, and as such, it carries zero mean curvature energy.

Now consider solutions with nonzero mean curvature in $r > 1$. A mean curvature field that is harmonic and square integrable (i.e., finite energy) has a multipole expansion whose leading term is quadrupole (Landau and Lifshitz, 1975):

$$\kappa = \frac{1}{r^2}(a_2\cos 2\theta + b_2\sin 2\theta) + \frac{1}{r^3}(a_3\cos 3\theta + b_3\sin 3\theta) + \cdots \tag{11}$$

This result appears in Appendix A. Biharmonic displacement fields, $z = h(\mathbf{x})$, consistent with the curvature field (Eq. 11) satisfy the Poisson equation

$$\nabla^2 h = 2\kappa = \frac{2}{r^2}(a_2\cos 2\theta + b_2\sin 2\theta) + \frac{2}{r^3}(a_3\cos 3\theta + b_3\sin 3\theta) + \cdots \tag{12}$$

The most general solution of (Eq. 12) that satisfies the boundary conditions of Eqs. 8 and 9 is

$$h = -\gamma \ln r + \frac{1}{2}\left\{\frac{1}{2}\left(r^2 + \frac{1}{r^2}\right) - 1\right\}(a_2\cos 2\theta + b_2\sin 2\theta) + \frac{1}{4}\left\{\frac{r^3}{3} + \frac{2}{3}\frac{1}{r^3} - \frac{1}{r}\right\}(a_3\cos 3\theta + b_3\sin 3\theta) + \cdots \tag{13}$$

The mean curvature energy associated with the displacement field (Eq. 13) is

$$\begin{aligned} E_m &= 2a\int_{r>1}\kappa^2 d\mathbf{x} \\ &= 2a\int_1^\infty\int_0^{2\pi}\frac{1}{r^4}(a_2\cos 2\theta + b_2\sin 2\theta)^2 r\, dr\, d\theta \\ &\quad + 2a\int_1^\infty\int_0^{2\pi}\frac{1}{r^6}(a_3\cos 3\theta + b_3\sin 3\theta)^2 r\, dr\, d\theta + \cdots \\ &= \pi a\left\{a_2^2 + b_2^2 + \frac{1}{2}(a_3^2 + b_3^2) + \cdots\right\}. \end{aligned} \tag{14}$$

Most of the energy is concentrated in an annulus of O(1) thickness about the protein. For instance, the energy density associated with the quadrupole term of mean curvature (Eq. 11) has radial dependence $1/r^4$, and the fraction of quadrupole energy in $1 < r < 2$ is $\int_1^2 (dr/r^3)/\int_1^\infty (dr/r^3) = 3/4$. For energies associated with higher multipole terms of Eq. 11, the fraction is even closer to unity.

It remains to place the solution to Eq. 13 within the framework of widely spaced proteins in a bilayer. A basic feature of the displacement field of Eq. 13 is the rapid $1/r^2$ decay of the associated mean curvature (Eq. 11). In the many-protein system, we expect that the mean curvature and associated energy density are similarly concentrated about the proteins. In the large expanse of the bilayer far from the proteins, the mean curvature is negligible, and, to leading order, the displacement field is approximated by a harmonic background field $\phi(\mathbf{x})$. Let **P** denote a point on the membrane far from a protein. Let $\{\mathbf{1_P}, \mathbf{2_P}, \mathbf{3_P}\}$ be Cartesian axes at the point **P**, with $\mathbf{1_P}$ and $\mathbf{2_P}$ in the tangent plane, as shown in Fig. 2.

The local behavior of $\phi(\mathbf{x})$ in a neighborhood of **P** small compared to interprotein distance is dominated by quadratic

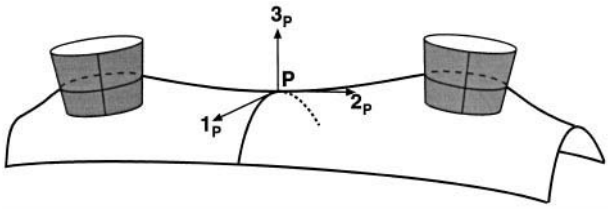

FIGURE 2 A Cartesian frame is adopted locally on the membrane at any point **P** that is far from a protein with $\mathbf{1_P}$ and $\mathbf{2_P}$ axes in the tangent plane.

terms

$$\phi \sim \frac{\alpha}{2}(x_1^2 - x_2^2) + \beta x_1 x_2 = \frac{r^2}{2}(\alpha \cos 2\theta + \beta \sin 2\theta), \tag{15}$$

where $\alpha \equiv \partial_{11}\phi(\mathbf{0}) = -\partial_{22}\phi(\mathbf{0})$, $\beta \equiv \partial_{12}\phi(\mathbf{0})$.

Now consider how the local structure of the displacement field is modified when a protein is introduced at the point **P**. In the limit of large interprotein distance, $l \gg 1$, the leading approximation to the displacement field takes the general form of Eq. 13. Note that Eq. 13 is not exact, because the associated mean curvature decays like $1/r^2$ as $r \to \infty$, and this ignores "curvature tails" originating from neighboring proteins. But in the limit of large interprotein distance the effect of these tails turns out to be negligible. The constants a_2, b_2, a_3, b_3, ... in Eq. 13 are identified by requiring an asymptotic matching between Eq. 13 and the background field (Eq. 15) in the "intermediate limit" $1 \ll r \ll l$. For $r \gg 1$, the dominant component of Eq. 13 is the harmonic function $(r^2/2^2)(a_2\cos 2\theta + b_2 \sin 2\theta) + (r^3/3^2)(a_3 \cos 3\theta + b_3 \sin 3\theta) + \cdots$, and agreement with Eq. 15 leads to

$$a_2 = 2\alpha \tag{16}$$

$$b_2 = 2\beta. \tag{17}$$

Coefficients a_3 and b_3 of the r^3 component are seen to be negligible, as are coefficients of the remaining higher powers of r. In summary, the local structure of displacement field about the protein at **P** is approximated by

$$h \approx -\gamma \ln r + \left\{\frac{1}{2}\left(r^2 + \frac{1}{r^2}\right) - 1\right\}(\alpha \cos 2\theta + \beta \sin 2\theta). \tag{18}$$

The energy cost of introducing the protein at **P** is

$$E_m \approx \pi a(a_2^2 + b_2^2) = 4\pi a(\alpha^2 + \beta^2). \tag{19}$$

This energy has a geometrical interpretation. The extrinsic curvature tensor of the neutral surface, $z = \phi(\mathbf{x})$, in the absence of a protein at **P** is

$$\kappa = \begin{pmatrix} \partial_{11}\phi & \partial_{12}\phi \\ \partial_{21}\phi & \partial_{22}\phi \end{pmatrix}. \tag{20}$$

Observe that

$$\kappa(\mathbf{x} = \mathbf{0}) = \begin{pmatrix} \alpha & \beta \\ \beta & -\alpha \end{pmatrix}$$

and $\det \boldsymbol{\kappa}(0) = -(\alpha^2 + \beta^2)$, so the energy of Eq. 19 can be written as

$$E_m \approx -4\pi a \det \boldsymbol{\kappa}(\mathbf{0}). \tag{21}$$

$\det \boldsymbol{\kappa}(\mathbf{0})$ approximates the Gaussian curvature of the surface $z = \phi(\mathbf{x})$ at $\mathbf{x} = \mathbf{0}$. Thus, the energy cost of introducing a protein at any point **P** of the bilayer is proportional to the preexisting Gaussian curvature at **P**.

To conclude this section, we mention some features of the long-range tails of the displacement field h. In the local structure (Eq. 18) of displacement field h, the component proportional to r^2 represents the preexisting saddle-shaped background configuration before the protein is introduced. The remaining terms that do not asymptote to zero as $r \to \infty$ contribute to the long-range behavior of displacement field far from a disk containing all of the proteins. Specifically, in Appendix D we show that the $r \to \infty$ tail of h has the generic form

$$h \approx -\Gamma \ln r - \frac{1}{2}(a_2 \cos 2\theta + b_2 \sin 2\theta) + O\left(\frac{1}{r}\right). \tag{22}$$

The coefficient Γ is given by $\Gamma = N\gamma$, where N is the number of proteins, so the harmonic $\ln r$ component is seen to be the direct effect of the contact angle γ associated with all of the proteins. The tail structure (Eq. 22) that does not asymptote to zero as $r \to \infty$ challenges the physical relevance of the unbounded bilayer solutions constructed in this paper. However, in Appendix D we consider an ensemble of proteins near the center of a large disk with a clamped perimeter. The clamped perimeter obviously modifies the tail structure (Eq. 22). But the effect on energy vanishes as the radius of the disk tends to infinity.

THE MANY-BODY PROBLEM

Suppose the background field in the previous section arises from a single protein at position $\mathbf{x}'$. This background field is approximated by the single-protein solution (Eq. 10) with r replaced by $|\mathbf{x} - \mathbf{x}'|$:

$$\phi = -\gamma \ln|\mathbf{x} - \mathbf{x}'|. \tag{23}$$

The energy cost of inserting a protein into the membrane at the origin is computed as follows. The extrinsic curvature tensor of the background field ϕ at $\mathbf{x} = \mathbf{0}$ is approximately

$$\kappa(\mathbf{0}) = \begin{pmatrix} \alpha & \beta \\ \beta & -\alpha \end{pmatrix}, \tag{24}$$

where

$$\alpha \equiv \partial_{11}\phi(\mathbf{0}) = -\partial_{22}\phi(\mathbf{0}) = \gamma \frac{x_1'^2 - x_2'^2}{(x_1'^2 + x_2'^2)^2}$$

$$\beta \equiv \partial_{12}\phi(\mathbf{0}) = \partial_{21}\phi(\mathbf{0}) = \gamma\frac{2x_1'x_2'}{(x_1'^2 + x_2'^2)^2}.$$

The formula for α, β suggests a complex variable notation. If we represent position $\mathbf{x}'$ by the complex number $z' = x_1' + ix_2'$, then the components α and β of the curvature tensor are contained in the complex curvature scalar:

$$\eta \equiv \alpha - i\beta = \gamma\frac{x_1'^2 - x_2'^2 - 2ix_1'x_2'}{(x_1'^2 + x_2'^2)^2} = \frac{\gamma\bar{z}'^2}{|z'|^4} = \frac{\gamma}{z'^2}. \quad (25)$$

Using this notation, the Gaussian curvature at the origin is represented by

$$\det \boldsymbol{\kappa}(\mathbf{0}) = \alpha^2 + \beta^2 = |\eta|^2, \quad (26)$$

and the energy cost of inserting a protein at the origin is

$$E_m = 4\pi a|\eta|^2. \quad (27)$$

From Eq. 25 this becomes

$$E_m = \frac{4\pi a\gamma^2}{|z'|^4}. \quad (28)$$

As remarked before, this mean curvature energy is concentrated in an annulus of thickness ~ 1 about the protein at $z = 0$. If a protein at z' is the only other protein present, there is a similar annulus with concentrated mean curvature energy about it, and the total energy of the two-protein system is

$$E_m = \frac{8\pi a\gamma^2}{r^4}, \quad r \equiv |z'|. \quad (29)$$

This circularly symmetrical, repulsive, $1/r^4$, two-body energy is the same as reported by Goulian et al. (1993). One might think that the repulsive character of the two-body interaction is due to the contact angle γ being the same for both proteins, analogous to repulsion between like charges. Suppose there are two proteins, 1 and 2, with contact angles γ_1, γ_2. The energy cost of protein 1 in the background field due to protein 2 is $4\pi a\gamma_2^2/r^4$, and the energy cost of protein 2 in the background field due to 1 is $4\pi a\gamma_1^2/r^4$, so the total energy of this two-protein system is

$$E_m = \frac{4\pi a(\gamma_1^2 + \gamma_2^2)}{r^4}. \quad (30)$$

Thus the two-body interaction is repulsive, irrespective of the relative signs of γ_1 and γ_2.

A straightforward extrapolation to $N \geq 3$ proteins would be to assume the sum of pairwise $1/r^4$ interactions. But a closer look at the formulation given here reveals the nonpairwise character of the interaction.

Suppose the background field $\phi(\mathbf{x})$ is due to $N - 1$ proteins at positions represented by complex numbers $z_2, \ldots, z_N$. The curvature scalar at the origin due to these proteins is approximated by the superposition of single protein curvature scalars,

$$\eta = \sum_{i=2}^{N}\frac{\gamma}{z_i^2}. \quad (31)$$

The energy cost of introducing a protein at the origin is now given by

$$4\pi a|\eta|^2 = 4\pi a\gamma^2\left|\sum_{i=2}^{N}\frac{1}{z_i^2}\right|^2. \quad (32)$$

If the interaction were pairwise, the energy cost would be

$$4\pi a\gamma^2\sum_{i=2}^{N}\frac{1}{|z_i|^4}, \quad (33)$$

corresponding to the $N - 1$ pairwise interactions between the protein at the origin and its $N - 1$ neighbors. The true energy cost (Eq. 32) contains all of the terms of Eq. 33, but many other cross terms as well. This establishes the true many-body character of the elastic interaction between proteins in the bilayer. The total mean curvature energy of N proteins at positions $z_1, \ldots, z_N$ consists of N terms like Eq. 32. The energy concentrated about the jth protein is approximately $4\pi a\gamma^2|\Sigma_{i\neq j}(1/(z_i - z_j)^2|^2$, and the total energy is approximately

$$E_m \approx 4\pi a\gamma^2\sum_{j=1}^{N}\left|\sum_{i\neq j}\frac{1}{(z_i - z_j)^2}\right|^2. \quad (34)$$

STABLE PROTEIN AGGREGATES

That the many-body energy (Eq. 34) is nonpairwise can be demonstrated by a simple example. Consider seven proteins, one at the origin and the other six at the vertices of a regular hexagon centered about the origin, as shown in Fig. 3. The energy cost of the protein at the origin is computed from the curvature scalar at $z = 0$ due to proteins at positions $z = re^{ik\pi/3}$, $k = 0, 1, \ldots, 5$:

$$\eta = \frac{\gamma}{r^2}\sum_{k=0}^{5}e^{i\frac{k2\pi}{3}} = \frac{\gamma}{r^2}\frac{1 - (e^{i(2\pi/3)})^6}{1 - e^{i(2\pi/3)}} = 0. \quad (35)$$

Hence the energy cost of the protein at the origin is zero. If the true many-body energy were pairwise, the energy cost

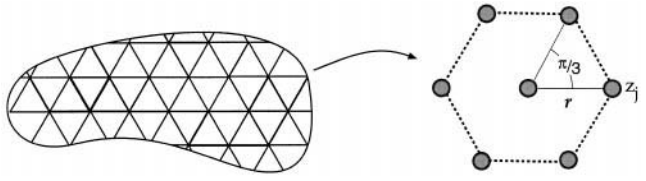

FIGURE 3 Configuration of seven proteins, with one at the origin and six at the vertices of a regular hexagon.

could be calculated as follows. Adding the protein at $z = 0$ introduces six new interactions between this protein and its six neighbors. The cost of each interaction is the pair energy (Eq. 29), and the total is $48\pi a\gamma^2/r^4$. It is evident that pairwise repulsive forces between proteins can be nullified by nonpairwise forces. This gives rise to an intriguing possibility: aggregates of proteins with N sufficiently large might self-assemble into truly stable equilibria. We demonstrate that such equilibria exist by numerically simulating the gradient flow generated by the mean curvature energy.

Let $\mathbf{X} \equiv (\mathrm{Re}\ z_1, \ldots, \mathrm{Re}\ z_N, \mathrm{Im}\ z_1, \ldots, \mathrm{Im}\ z_N)$ be a $2N$-dimensional vector that specifies the N protein positions in the reference plane, and define $E_m(\mathbf{X})$ to be the mean curvature energy given by Eq. 34. The gradient flow associated with $E_m(\mathbf{X})$ is the system of ordinary differential equations,

$$\frac{d\mathbf{X}}{dt} = -\nabla E_m(\mathbf{X}). \tag{36}$$

Here the gradient is with respect to the $2N$ vector $\mathbf{X}$. It follows from Eq. 36 that $dE_m(\mathbf{X}(t))/dt = \nabla E_m \cdot d\mathbf{X}/dt = -|\nabla E_m|^2 \leq 0$, with equality only if $\nabla E_m = 0$. If the time sequence $\mathbf{X}(t)$ converges as $t \to \infty$, then its limit $\mathbf{X}_\infty$ represents an equilibrium of the energy $E_m(\mathbf{X})$, satisfying

$$\nabla E_m(\mathbf{X}_\infty) = 0. \tag{37}$$

For the energy (Eq. 34), it can be shown that an equilibrium state satisfying Eq. 37 must also satisfy

$$E_m(\mathbf{X}_\infty) = 0. \tag{38}$$

This results from the homogeneity of the energy (Eq. 34). In particular, suppose that $\mathbf{X}_\infty$ is a solution of Eq. 37. It follows from Eq. 34 that $E_m(l\mathbf{X}_\infty) = (1/l^4)E_m(\mathbf{X}_\infty)$. Taking d/dl of both sides and setting $l = 1$, $\nabla E_m(\mathbf{X}_\infty) \cdot \mathbf{X}_\infty = -4E_m(\mathbf{X}_\infty)$. Because $\nabla E_m(\mathbf{X}_\infty) = 0$, it follows that $E_m(\mathbf{X}_\infty) = 0$. Given an equilibrium configuration $\mathbf{X}_\infty$ that satisfies Eq. 38, it may be further deduced from Eq. 34 that the curvature scalar η_i felt at each protein position z_i vanishes. Hence equilibria satisfy the N simultaneous equations

$$\eta_i = 0, \quad i = 1, \ldots, N. \tag{39}$$

All of the following simulations were performed over the same time interval. The first simulation in Fig. 4 consists of $N = 61$ proteins. The initial positions fill out a hexagonal lattice with four concentric "layers." The initially hexagonal lattice was motivated by the hope that it is near equilibrium; i.e., curvature scalars at sites away from the periphery should be nearly zero. Hence we expected that the hexagonal lattice sufficiently far from the periphery would retain its integrity for some time. We also expected that this lattice patch would "evaporate" from the edge, because we did not expect that small rearrangements of "boundary" proteins would lead to the vanishing of their curvature scalars, η_i.

If the final positions are a good approximation to an equilibrium, the curvature scalars at the final lattice sites (Fig. 4, *open circles*) should be close to zero. In Fig. 4, some

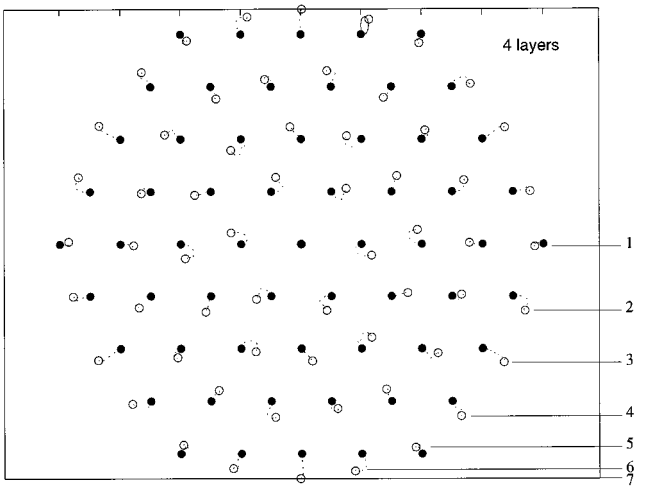

FIGURE 4 $N = 61$ protein lattice simulation. The initial positions are represented by black dots, and the positions of the proteins at the end of the run are represented by open circles. The final and initial values of $|\eta_i|$ at seven selected boundary proteins (labeled from 1 to 7) are as follows: (1) 0.0008 (2.3051); (2) 0.0008 (0.3221); (3) 0.0008 (0.1111); (4) 0.0008 (0.3221); (5) 0.0018 (2.3051); (6) 0.0008 (0.3221); (7) 0.0008 (0.1111).

representative "boundary" proteins are labeled 1–7. The figure caption lists final and initial values (in parentheses) of $|\eta_i|$, respectively, for each of these seven proteins. The final values of the curvature scalars at these boundary proteins are small relative to their initial values and are close to zero.

If one examines the trajectories of the proteins more closely, some of the proteins appear to move toward the center of the aggregate, as if they were experiencing an effective attraction. There also appears to be interesting rotation and counterrotation of the interior layers, hinting at the existence of symmetry-breaking instabilities and the formation of grain boundaries. The details of the final equilibrium are rich and subtle and will be a subject of analysis in a future publication. For now, notice that the final lattice has macroscopically "rounded" itself out into a circle from its initial hexagonal shape. Thus the original hexagonal lattice structure has been disrupted. This disruption is modest, for the final lattice sites are generally within a third of a lattice spacing of the initial sites. But the disruptions are not confined to a "boundary layer"; rather, they propagate throughout the entire patch and have many interesting symmetries.

A single pair of proteins undergoes indefinite expansion. A single hexagonal "layer" around a central protein also undergoes indefinite expansion, but more slowly. On the other hand, the four-layer patch of Fig. 4 settles down to an equilibrium. So what happens to two- and three-layer patches? Is there a critical layering size from which equilibrium can still be achieved? The simulations displayed in Fig. 5 were all carried out within the same time span; they indicate equilibration in both cases. The protein trajectories for smaller lattices as determined by the numerical gradient flow are shown as dotted curves in Fig. 5 *a* and *b*. Succes-

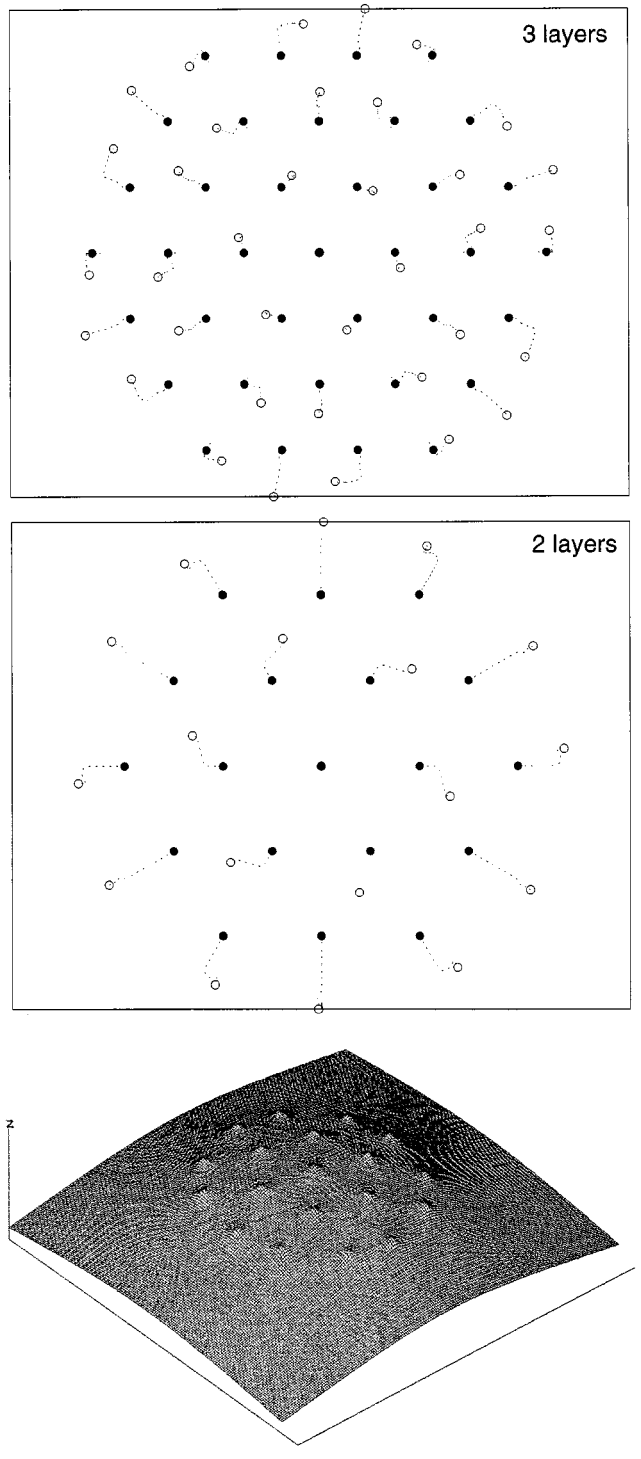

FIGURE 5 Simulation of three concentric layers (*a*) and two concentric layers (*b*). The two simulations were performed within the same time span. (*c*) membrane shape of the two-layer system at its final configuration.

sive dots represent equal increments of time. Notice that the dots cluster tightly together as the proteins settle down into an apparent equilibrium. We shall show below that five proteins at the vertices of any regular pentagon constitute a stable equilibrium.

It is of interest to compare the gradient flow of the nonpairwise energy (Eq. 34) with that of the pairwise energy

$$E_p = 4\pi a\gamma^2 \sum_{i\neq j} \frac{1}{|z_i - z_j|^4}. \tag{40}$$

Fig. 6 shows the expansion of the two-layer configuration driven only by the pairwise gradient force. In dramatic contrast to the nonpairwise case, the lattice patch expands radially outward.

We can approximate the expansion rate of the array as follows. The numerical solution does not exactly represent a uniform dilation of the whole lattice, but it is not a bad approximation. Let us approximate the real evolution $\mathbf{X}(t)$ by $\mathbf{X}(t) \approx l(t)\mathbf{X}_0$, where $\mathbf{X}_0$ is the initial configuration, so $l(0) = 1$. Using the homogeneity of the pairwise energy (Eq. 40), an ordinary differential equation for $l(t)$ is obtained by taking the inner product of the full gradient flow equation with initial condition $\mathbf{X}_0$ and substituting the above approximation for $\mathbf{X}$:

$$\frac{dl}{dt} = -\frac{-4E_p(\mathbf{X}_0)}{|\mathbf{X}_0|^2}\frac{1}{l^5}. \tag{41}$$

From Eq. 41 it easily follows that $l(t) \sim (\text{constant})t^{1/6}$ as $t \to \infty$. Fig. 7 shows a log-log plot of the diameter of the lattice patch versus time, for both pairwise and nonpairwise simulations. The pairwise slope is much greater than the nonpairwise examples, and the discrepancy jumps by orders of magnitude as each concentric layer is added, lending further evidence of the stabilizing influence of the nonpairwise forces.

Why do the curvature scalars at boundary lattice sites manage to vanish, even though a boundary protein sits at a place where spatial homogeneity is broken? Recall our calculation (Eq. 35), which showed that the protein at the

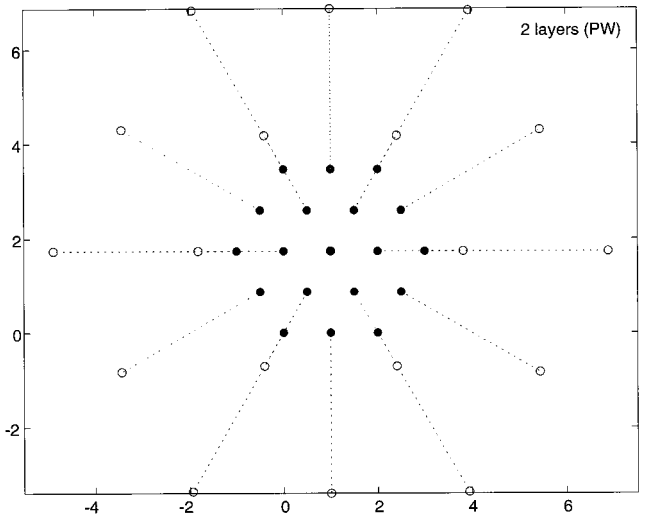

FIGURE 6 Simulation of 19 proteins in an initially hexagonal array driven by the gradient of the pairwise energy (40). The initial pattern rapidly expands radially, compared to the same initial condition in Fig. 5 *b*.

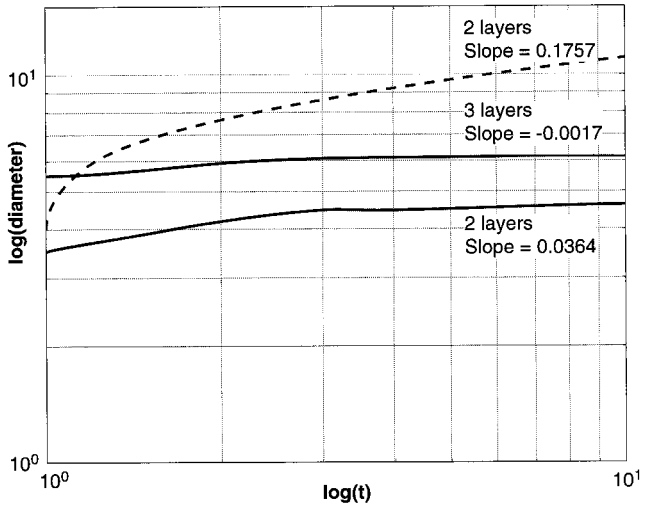

FIGURE 7 Log-log plot of the diameter of the protein patch versus time when driven by pairwise and nonpairwise forces. The curves show the expansion rate of two concentric layers driven by pairwise forces, and plots for two and three layers driven by nonpairwise forces. For the pairwise simulation, the log-log plot has slope 0.1757 at the end of the run, close to the predicted value of 1/6. For the two-layer and three-layer nonpairwise dynamics, the final slopes are 0.0364 and −0.0017, respectively.

center of a hexagonal array feels zero curvature scalar due to its six nearest neighbors. To obtain zero curvature scalar at the center protein, one does not need to sum over all six nearest neighbors; any consecutive three will do. Fig. 8 illustrates this example. We can imagine that a boundary protein is at $z = 0$, and its three nearest neighbors at $z = l$, $le^{i\pi/3}$, $le^{i2\pi/3}$ can be part of the interior and/or boundary of the aggregate. It is easily seen that the boundary protein at $z = 0$ has a vanishing curvature scalar due to these interior and/or boundary proteins.

Because the nonpairwise interaction we have derived possesses interesting symmetry properties, it is now less mysterious that a protein on the boundary of a lattice patch can have zero curvature scalar, even though it has no interacting partners on one half-plane and a sea of proteins on the other. Thus a boundary protein adds to the overall stability of the aggregate.

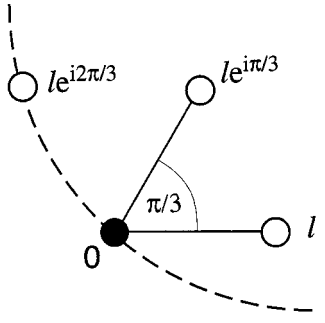

FIGURE 8 The curvature scalar at $z = 0$ due to proteins at $z = l$, $le^{i\pi/3}$, $le^{i2\pi/3}$ vanishes.

PENTAGONS ARE THE SMALLEST STABLE PROTEIN AGGREGATE

We will now show that five proteins at the vertices of a regular pentagon represent a zero-energy equilibrium state. The protein positions are taken to be

$$z_j = r\omega^j, \quad j = 0, 1, \ldots, 4, \tag{42}$$

where $\omega \equiv e^{2\pi i/5}$.

The configuration is shown in Fig. 9. The curvature scalar at $z_0 = 1$ due to proteins at $z_1, \ldots, z_4$ is

$$\eta = \frac{\gamma}{r^2}\left\{\frac{1}{(\omega - 1)^2} + \frac{1}{(\omega^2 - 1)^2} + \frac{1}{(\bar{\omega}^2 - 1)^2} + \frac{1}{(\bar{\omega} - 1)^2}\right\}. \tag{43}$$

Here we used $\omega^3 = \bar{\omega}^2$, $\omega^4 = \bar{\omega}$. Further use of these identities and an algebraic rearrangement of Eq. 43 give

$$\eta = \frac{2\gamma}{r^2}\frac{1}{|\omega - 1|^2}\,\mathrm{Re}\{3(\omega^2 - \bar{\omega}^2) + (\omega - \bar{\omega})\} = 0. \tag{44}$$

Hence the energy cost of the protein at $z_0 = 1$ is zero. Curvature scalars at the other protein sites and energy costs of the remaining proteins are also zero by geometric symmetry. In Appendix E we show that these pentagonal configurations of proteins are the smallest possible aggregate. In Appendix F we give a precise definition of "geometric stability" that enables us to discuss unambiguously whether equilibrium configurations such as the ones we observed in Figs. 4 and 5 are stable.

DISCUSSION

The phenomena motivating this work are the aggregation of identical proteins in biological cell membranes. We have focused our attention on protein-protein interactions that are mediated by elastic deformations of the membrane. Proteins

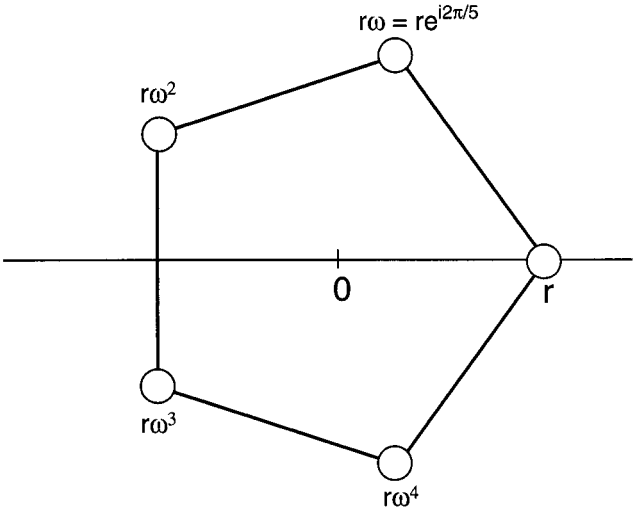

FIGURE 9 A pentagonal protein aggregate.

embedded in the bilayer induce curvature distortions that are resisted by the elastic restoring forces of the membrane. These deformations can be imposed externally or induced by the proteins themselves. Thus a protein interacts with its neighboring proteins via the local membrane curvature generated by its neighbors.

Goulian et al. derived a purely elastic interaction between two proteins at zero temperature, with a circularly symmetrical, repulsive potential energy that diminished as $1/r^4$ (Goulian et al., 1993). At positive temperatures, this potential energy can be either attractive or repulsive, depending on the relative rigidities of the protein and the membrane (Goulian et al., 1993; Park and Lubensky, 1996). In this paper we have shown that curvature-mediated protein interactions are not pairwise additive, and we have derived the correct interaction potential. Each protein feels a local curvature that is a linear superposition of curvatures due to neighbors. The energy of each protein is the square of this local curvature; hence the energy of a large protein ensemble has the structure

$$\text{Curvature elastic energy} = \sum_{\text{proteins}} \Big| \sum_{\text{neighbors}} (\text{curvatures})\Big|^2.$$

It is easy to see that such an energy does not reduce to a sum of pairwise energies.

The nonpairwise character of curvature-mediated protein interactions has novel implications for large protein assemblies. If the interaction were pairwise and repulsive, a local concentration of proteins would simply expand over an ever increasing area. But for nonpairwise interactions, the proteins in a large assembly can arrange themselves into a lattice such that at each of the lattice sites inside the assembly, the local curvature felt at that site due to all other proteins vanishes by cancellation. Thus all proteins in the assembly have zero energy. The assembly of five proteins into a regular pentagon is the simplest example. In our numerical simulations of the curvature energy gradient flow, larger aggregates relax to stable equilibria. In these examples the final aggregate size is about the same as the initial size. This is completely unlike the uniform expansion seen in protein aggregates interacting through pairwise forces. In fact, one can deduce from these results that the magnitude of the nonpairwise forces in the lattice patch is opposite and equal to that of the pairwise forces. This is in contrast to other nonpairwise forces found in nature, such as van der Waals forces, that have nonpairwise contributions that are usually small compared to the pairwise interactions.

Thus our work illustrates an example of how peculiar and counterintuitive nonpairwise forces behave, especially in their ability to stabilize large aggregates, even though isolated pairs of constituent bodies interact repulsively. We will demonstrate in a subsequent publication that the phenomena discussed here survive in the presence of thermal fluctuations of the proteins and of the membrane.

APPENDIX A: THE RELATIONSHIP BETWEEN ELASTIC ENERGY, FORCES, AND TORQUES IN A BIHARMONIC FIELD

This appendix analyzes forces and torques associated with the mean curvature energy (Eq. 4). The starting point is the biharmonic Green's identity. Let $g(\mathbf{x})$ and $h(\mathbf{x})$ be scalar fields defined in $\mathbf{s}$. Integrating the vector identity

$$\nabla \cdot [\nabla^2 h \nabla g - \nabla(\nabla^2 h) g] = \nabla^2 h \nabla^2 g - \nabla^4 h g \quad \text{(A.1)}$$

over a region in $\boldsymbol{\sigma}$ contained in $\mathbf{s}$, and using the divergence theorem, one obtains

$$-\int_{\partial\sigma} [\nabla^2 h g_{\mathrm{n}} - (\nabla^2 h)_{\mathrm{n}} g]\mathrm{d}s = \int_{\sigma} \nabla^2 h \nabla^2 g \, \mathrm{d}\mathbf{x} - \int_{\sigma} \nabla^2 h g \, \mathrm{d}\mathbf{x}. \quad \text{(A.2)}$$

Here, normal derivatives, $(\bullet)_{\mathrm{n}} = \nabla(\bullet) \cdot \hat{\mathbf{n}}$, are with respect to the unit normal $\hat{\mathbf{n}}$ pointing into the region $\boldsymbol{\sigma}$.

We first apply Eq. A.2 to compute the variations of the mean curvature energy (Eq. 5). The variation of E_{m} due to variations in δh in $\mathbf{s}$ is

$$\delta E_{\mathrm{m}} = a \int_{\mathrm{s}} \nabla^2 h \nabla^2 \delta h \, \mathrm{d}\mathbf{x}. \quad \text{(A.3)}$$

Now set $g = \delta h$ and $\boldsymbol{\sigma} = \mathbf{s}$ in (A.2):

$$\int_{\mathrm{s}} \nabla^2 h \nabla^2 \delta h \, \mathrm{d}\mathbf{x} = \int_{\mathrm{s}} \nabla^4 h \delta h \, \mathrm{d}\mathbf{x} - \int_{\partial \mathrm{s}} [\nabla^2 h \delta h_{\mathrm{n}} - (\nabla^2 h)_{\mathrm{n}} \delta h]\mathrm{d}s. \quad \text{(A.4)}$$

Comparison with (A.3) leads to

$$\delta \mathbf{E}_{\mathrm{m}} = a \int_{\mathrm{s}} \nabla^4 h \delta h \, \mathrm{d}\mathbf{x} - a \int_{\partial \mathrm{s}} [\nabla^2 h \delta h_{\mathrm{n}} - (\nabla^2 h)_{\mathrm{n}} \delta h]\mathrm{d}s. \quad \text{(A.5)}$$

We can interpret this variation formula in terms of the forces and torques.

Consider the area integral over $\mathbf{s}$ in (A.5). The integrand, $a\nabla^4 h \delta h \, \mathrm{d}\mathbf{x}$, is the work required to raise the patch of bilayer over area element $\mathrm{d}\mathbf{x}$ by height δh. Hence this patch of bilayer is subject to a vertical restoring force $-a\nabla^4 h$ per unit area. This force vanishes for bilayer configurations in local mechanical equilibrium. Hence $h(\mathbf{x})$ must satisfy the biharmonic equation $\nabla^4 h = 0$ in $\mathbf{s}$.

The boundary integral in Eq. A.5 encodes vertical forces and horizontal torques acting on the proteins.

The balance of vertical forces on a protein

If the protein is raised vertically by amount δz with no rotation, every point on the protein-bilayer contact curve, $\mathbf{c}$, translates upward uniformly by δz; so $\delta h = \delta z$ on $\mathbf{c}$. The tangent planes along $\mathbf{C}$ also undergo uniform upward translation, so $\delta h_{\mathrm{n}} = 0$ on $\mathbf{c}$. In this case the boundary integral in Eq. A.5 reduces to $a\int_{\mathrm{c}} (\nabla^2 h)_{\mathrm{n}} \mathrm{d}s \, \delta z$, where $\mathbf{c}$ is the projection of $\mathbf{C}$ and is thus one of the closed curves of $\partial\mathbf{s}$ corresponding to a single protein. This integral represents the work required to raise the protein by amount δz against a

vertical restoring force:

$$f_c \equiv -a \int_c (\nabla^2 h)_n ds. \tag{A.6}$$

The balance of horizontal torques on a protein

Next consider the work done on the bilayer by pivoting the protein about some horizontal axis. Such a pivoting motion is represented by

$$\delta h = (\mathbf{J} \cdot \mathbf{w}) \cdot \mathbf{x} \tag{A.7}$$

on **c**. Here, **w** is a small vector in the direction of the rotation axis through a pivot of θ, as shown in

$$\mathbf{J} = \begin{pmatrix} 0 & -1 \\ 1 & 0 \end{pmatrix}$$

is the rotation matrix by $+\pi/2$ radians in the horizontal plane. Such a pivoting motion changes the projection of the protein-bilayer contact curve, **C**, onto the reference plane, but we can neglect this effect for the near planar configurations considered here. Substituting Eq. A.7 for δh into the boundary integral in Eq. A.5 gives

$$-\int_c [(\nabla^2 h \mathbf{J}\mathbf{w} \cdot \hat{\mathbf{n}} - (\nabla^2 h)_n \mathbf{J}\mathbf{w} \cdot \mathbf{x})] ds = \left[a \int_c [(\nabla^2 h \hat{\mathbf{t}} - (\nabla^2 h)_n \mathbf{J}\mathbf{x})] ds \right] \cdot \mathbf{w}.$$

Here $\hat{\mathbf{t}}$ is the unit tangent of **c**, oriented counterclockwise. This integral represents the work that must be supplied to carry out the pivoting **w**. Hence there is a restoring torque applied by the bilayer to the protein, given by

$$\boldsymbol{\tau}_C \equiv -a \int_c (\nabla^2 h \hat{\mathbf{t}} - (\nabla^2 h)_n \mathbf{J}\mathbf{x}) ds. \tag{A.8}$$

Because the mean curvature is given by $\kappa(\mathbf{x}) = 1/2\nabla^2 h(\mathbf{x})$ in the small deflection limit, the formulas A.6 and A.8 for vertical force and horizontal torque imposed by the bilayer upon the protein can be written as

$$\text{vertical force:} \quad f_C = -2a \int_c \kappa_n \, ds \tag{A.9}$$

$$\text{horizontal torque:} \quad \boldsymbol{\tau}_C = -2a \int_c (\kappa \hat{\mathbf{t}} - \kappa_n J\mathbf{x}) ds. \tag{A.10}$$

Unbounded bilayer and the equilibrium of forces and torques

For an equilibrium biharmonic displacement field $h(\mathbf{x})$ in **s** with finite mean curvature energy, the vertical elastic forces and the horizontal torques on all proteins must sum to zero. We show this as follows.

Let $\kappa(\mathbf{x}) = \frac{1}{2}\nabla^2 h(\mathbf{x})$ be the mean curvature associated with a biharmonic displacement field $h(\mathbf{x})$. As noted in the second section, κ is harmonic, and setting $\nabla^2 h = 2\kappa$ in the biharmonic green's identity (Eq. A.2) gives

$$-\int_{\partial\sigma} (\kappa g_n - \kappa_n g) ds = \int_\sigma \kappa \nabla^2 g \, d\mathbf{x}. \tag{A.11}$$

Here g remains an arbitrary test function as yet unspecified, and the region $\boldsymbol{\sigma}$ is the portion of **s** inside a circle $\mathbf{c}_r$ of radius r about the origin. r is chosen sufficiently large so that all proteins are enclosed inside $\mathbf{c}_r$, as shown in Fig. 10.

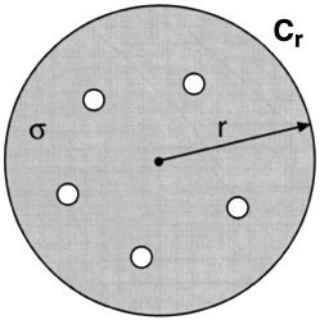

FIGURE 10 A region σ enclosed by $\mathbf{c}_r$.

Recall that $\partial\mathbf{s}$ consists of the closed curves corresponding to all of the proteins, and that all of these are inside $\mathbf{c}_r$. Hence, $\partial\boldsymbol{\sigma} = \partial\mathbf{s} + \mathbf{c}_r$, and Eq. A.11 can be rewritten as

$$-\int_{\partial s} (\kappa g_n - \kappa_n g) ds = \int_{c_r} (\kappa g_r - \kappa_r g) ds + \int_\sigma \kappa \nabla^2 g d\mathbf{x}. \tag{A.12}$$

Notice that the normal derivative is $-\partial/\partial r$ on $\mathbf{c}_r$, according to the convention discussed before. If g is taken to be a uniform constant, then $\nabla^2 g = 0$, and Eq. A.12 reduces to

$$\int_{\partial s} \kappa_n \, ds = \int_{c_r} \kappa_r \, ds. \tag{A.13}$$

The left-hand side is proportional to the sum of vertical elastic forces over all proteins, and it remains to show that the right-hand side vanishes as $r \to \infty$.

Because we have imposed the constraint that the total mean curvature energy (Eq. 5) is finite, the mean curvature field, κ, is square integrable over **s**. It follows that κ must vanish as $r \to \infty$. Because κ is harmonic, its behavior for large r can be described by a multipole expansion:

$$\kappa = \frac{1}{r}(a_1 \cos\theta + b_1 \sin\theta) + \frac{1}{r^2}(a_2 \cos 2\theta + b_2 \sin 2\theta) + \cdots \tag{A.14}$$

Here (r, θ) are polar coordinates in the plane, and the $1/r$ terms are dipole components. If there is a nonzero dipole component, then $\kappa^2 = O(1/r^2)$ as $r \to \infty$, but this decay is not rapid enough for square integrability on **s**. If the first nonzero term of Eq. A.13 is the quadrupole, then $\kappa^2 = O(1/r^4)$, and this decay is sufficient to ensure that κ^2 is square integrable on **s**. In addition, note that

$$\kappa = O\left(\frac{1}{r^2}\right) \quad \text{and} \quad \kappa_r = O\left(\frac{1}{r^3}\right) \quad \text{as } r \to \infty. \tag{A.15}$$

From Eq. A.15 we see that the right-hand side of Eq. A.14 is on the order of $O(1/r^2)$ as $r \to \infty$, so it vanishes as $r \to \infty$. Hence the sum of vertical forces on all proteins vanishes.

If g is taken to be a linear function, $g = J\mathbf{w} \cdot \mathbf{x}$, with $\mathbf{w}$ an arbitrary constant vector, then $\nabla^2 g$ is still zero, and Eq. A.12 reduces to

$$\mathbf{w} \cdot \int_{\partial s} (\kappa \hat{\mathbf{t}} - \kappa_n \mathbf{J}\mathbf{x}) \mathrm{d}s = \mathbf{w} \cdot \int_{c_r} r(\kappa - r\kappa_r)\hat{\boldsymbol{\theta}}\, \mathrm{d}\theta. \quad \text{(A.16)}$$

By Eq. A.15 the right-hand side is $O(1/r)$ as $r \to \infty$. Hence,

$$\mathbf{w} \cdot \int_{\partial s} (\kappa \hat{\mathbf{t}} - \kappa_n \mathbf{J}\mathbf{x}) \mathrm{d}s = 0. \quad \text{(A.17)}$$

This identity is true for arbitrary $\mathbf{w}$, so

$$\int_{\partial s} (\kappa \hat{\mathbf{t}} - \kappa_n \mathbf{J}\mathbf{x}) \mathrm{d}s = 0. \quad \text{(A.18)}$$

Thus the sum of horizontal torques over all proteins vanishes.

APPENDIX B: ANALYSIS OF VERTICAL FORCES AND HORIZONTAL TORQUES

The energy divergences associated with unbalanced vertical forces and horizontal torques will now be examined more concretely in simple examples. These will explain why imposing force and torque balances on each protein, as well as on the whole ensemble, is physically justified.

Consider the mean curvature field induced by vertical forces on proteins. Recall that the mean curvature field is harmonic (Eq. 7) and that the vertical force f_c induced on a protein by the surrounding bilayer is given by A.9. By Newton's third law, the protein exerts vertical forces $-f_c$ on the bilayer. This will lead to the interpretation of the vertical force $-f_c$ as a "source" of the mean curvature field. Suppose that the interprotein distances are large compared to the protein radius, so vertical forces may be considered as acting at discrete points corresponding to protein positions $\mathbf{x}_1, \ldots, \mathbf{x}_N$. Let $-f_1, \ldots, -f_N$ be forces applied to the bilayer at these points. Equations 7 and A.9 are replaced by the single Poisson equation

$$2a\nabla^2 \kappa = -\sum_{i=1}^{N} f_i \delta(\mathbf{x} - \mathbf{x}_i). \quad \text{(B.1)}$$

A particular solution of Eq. B.1 is

$$2a\kappa = -\frac{1}{2\pi} \sum_{i=1}^{N} f_i \ln|\mathbf{x} - \mathbf{x}_i|, \quad \text{(B.2)}$$

and the general solution is obtained by the addition of an arbitrary harmonic function. If the displacement field is to be asymptotically flat at infinity, then the additive harmonic function must be identically zero, and it is sufficient to consider Eq. B.2 as it stands. The asymptotic behavior of Eq. B.2 as $r \equiv |x| \to \infty$ is

$$2a\kappa \approx -\frac{1}{2\pi}\left(\sum_{i=1}^{N} f_i\right) \ln r + \frac{1}{2\pi}\left(\sum_{i=1}^{N} f_i \mathbf{x}_i\right) \cdot \frac{\hat{\mathbf{r}}}{r} + O\left(\frac{1}{r^2}\right). \quad \text{(B.3)}$$

For the mean curvature energy density $2a\kappa^2$ to be integrable at infinity, the sum of forces must vanish, and so must the horizontal torque,

$$\boldsymbol{\tau} \equiv \mathbf{J} \sum_{i=1}^{N} f_i x_i. \quad \text{(B.4)}$$

So far, this simple analysis recapitulates the conclusions of Appendix A, that asymptotic flatness at infinity and finite mean curvature energy imply balances of vertical forces and horizontal torques. We want to proceed further, and explain why the net vertical force on each protein should be taken as zero, i.e., $f_i = 0$ for $i = 1, \ldots, N$. Consider, for instance, three cylindrical proteins along a line, with spacing $l \gg 1$. The situation is depicted in Fig. 11.

Force $+f$ is applied to the outer proteins, and force $-2f$ to the protein in the middle. Force and torque balances are satisfied. Representing positions in the reference plane by complex numbers z, protein positions may be taken as $-l$, 0, $+l$, and the mean curvature field far from proteins is given by

$$2a\kappa \sim -\frac{f}{2\pi}\ln|z + l| + \frac{f}{\pi}\ln|z| - \frac{f}{2\pi}\ln|z - l|$$

$$= -\frac{f}{2\pi}\ln\left|1 - \frac{l^2}{z^2}\right| \quad \text{(B.5)}$$

The corresponding approximation to the total mean curvature energy is

$$E'_m \approx 2a \int_{\mathbf{R}^2} \kappa^2 \mathrm{d}\mathbf{x} = \frac{f^2}{8\pi^2 a} \int_s \ln^2 \left|1 - \frac{l^2}{z^2}\right| \mathrm{d}\mathbf{x}. \quad \text{(B.6)}$$

The singularities at $z = -l, 0, l$ are integrable, so E'_m in Eq. B.6 is finite and is in fact a leading order approximation to mean curvature energy in limit $l \to \infty$. By scaling the integration variables so that the scaled interprotein distance is unity, E'_m in Eq. B.6 can be rewritten as

$$E'_m \approx \mu f^2 l^2, \quad \text{(B.7)}$$

where μ is the constant $\mu \equiv (1/8\pi^2 a)\int_{\mathcal{R}^2} \ln^2|1 - (1/z^2)|\mathrm{d}\mathbf{x}$.

The energy in Eq. B.7 is compared with the curvature-mediated interaction energy given by Eq. 34. For three proteins at $-l$, 0, l, Eq. 34 reduces to

$$E_m = 4\pi a \gamma^2 \left\{ \left(\frac{2}{l^2}\right)^2 + 2\left(\frac{1 + \frac{1}{4}}{l^2}\right)^2 \right\} = \frac{57\pi}{2} \frac{a\gamma^2}{l^4}. \quad \text{(B.8)}$$

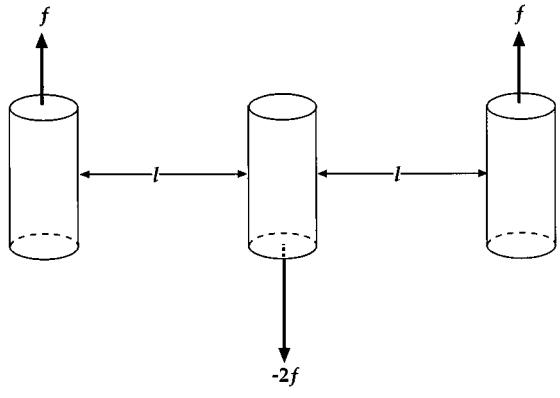

FIGURE 11 Three cylindrical proteins along a line illustrating force and torque balance.

The ratio E'_m/E_m scales with l like l^6, so $E'_m \gg E_m$ for $l \gg 1$. This result seems inevitable when one thinks of the length scales associated with the elastic distortions. Recall that the elastic distortions giving rise to the curvature interaction E_m in Eq. B.8 are confined mainly to annuli of thickness unity about each protein. The elastic distortions induced by vertical forces f, $-2f$, f on the three proteins at $-l$, 0, l are "transmitted" throughout a patch of radius $O(l)$ about the origin. The associated energy E'_m is bound to be enormous compared to E_m. Under any reasonable model of elastic relaxation, one expects that the highest energy modes undergo the fastest decay. In particular, the membrane should rapidly adjust itself so that the vertical force on each protein is zero.

There are energy divergences induced solely by torque. Consider a single circular protein in an otherwise unbounded bilayer. As before, let r, θ be polar coordinates of the reference plane, with $r > 1$ corresponding to the bilayer. Recall that the mean curvature field κ in $r > 1$ has a multipole expansion. If the curvature vanishes at infinity, the leading term is dipole. Assume that κ consists solely of the dipole term, so

$$\kappa = \frac{a_1}{r}\cos\,\theta, \tag{B.9}$$

where a_1 is a constant. The net vertical force on the protein vanishes, but the net torque horizontal torque is

$$-2a\int_0^{2\pi}(\kappa\hat{t} - \kappa_r\mathbf{J}\mathbf{x})|_{t=1}\mathrm{d}\theta = -4aa_1\int_0^{2\pi}\cos^2\theta\,\mathrm{d}\theta = -4\pi a a_1\mathbf{2} \equiv \tau_C\mathbf{2}. \tag{B.10}$$

If $a_1 \neq 0$, the torque $\tau_c = -4\pi a a_1$ is nonzero. A coordinate free expression of the dipole field (Eq. B.9) is convenient for the discussion of energetics. Points in the reference plane will be represented by the complex numbers z. The dipole field (Eq. B.9) can be written as

$$\kappa = a_1\mathrm{Re}\left(\frac{1}{z}\right) = -\frac{\tau_C}{4\pi a}\mathrm{Re}\left(\frac{1}{z}\right). \tag{B.11}$$

If the protein is located at a position ζ in the complex plane, the curvature field is

$$\kappa = -\frac{\tau_C}{4a\pi}\,\mathrm{Re}\left(\frac{1}{z-\zeta}\right). \tag{B.12}$$

The energy density $2a\kappa^2$ associated with this dipole field is nonintegrable at infinity. Now introduce a second protein at position $-\zeta$ with torque $-\tau_c\mathbf{2}$ imposed upon it. The sum of torques on the two proteins is now zero. If $|\zeta| \gg 1$, the mean curvature field due to both proteins together is approximated by the superposition

$$\kappa = -\frac{\tau_C}{4\pi a}\,\mathrm{Re}\left(\frac{1}{z-\zeta} - \frac{1}{z+\zeta}\right) = -\frac{\tau_C}{4\pi a}\,\mathrm{Re}\left(\frac{\zeta}{z^2-\zeta^2}\right). \tag{B.13}$$

As $|z| \to \infty$, $\kappa = O(1/|z|^2)$, and the mean curvature energy is finite:

$$E'_m \equiv 2a\int_{\boldsymbol{\sigma}}\kappa^2\mathrm{d}\mathbf{x} = \frac{\tau_C^2}{8\pi^2 a}\int_{\boldsymbol{\sigma}}\mathrm{Re}^2\left(\frac{l}{z^2-l^2}\right)\mathrm{d}\mathbf{x} < \infty \tag{B.14}$$

is finite. Here $\boldsymbol{\sigma}$ is the complex plane excluding the disks $|z-\zeta| < 1$, $|z+\zeta| < 1$.

The asymptotic behavior of this energy as $|\zeta| \to \infty$ is determined. The integration variables may be scaled so that the protein positions are $+1$ and -1. The resulting expression for E'_m is

$$E'_m = E'_m(\zeta) = \frac{\tau_C^2}{8\pi^2 a}\int_{\boldsymbol{\sigma}(\zeta)}\mathrm{Re}^2\left(\frac{1}{z^2-1}\right)\mathrm{d}\mathbf{x}, \tag{B.15}$$

where $\boldsymbol{\sigma}(\zeta)$ is the complement of disks $|z-1| < 1/|\zeta|$, $|z+1| < 1/|\zeta|$. Consider the change in E_m as $|\zeta|$ increases from some base value $\zeta_0 \gg 1$ to a final value $\zeta_1 > \zeta_0$. It follows from Eq. B.15 that

$$E'_m(\zeta_1) - E'_m(\zeta_0) = \frac{\tau_C^2}{8\pi^2 a}\int_{\mathbf{a}}\mathrm{Re}^2\left(\frac{1}{z^2-1}\right)\mathrm{d}\mathbf{x}, \tag{B.16}$$

where $\mathbf{a} \equiv \boldsymbol{\sigma}(\zeta_1) - \boldsymbol{\sigma}(\zeta_0)$. $\mathbf{a}$ consists of two annuli about $z = -1$ and $z = +1$ with inner radius $1/\zeta_1$ and outer radius $1/\zeta_0$.

In the annulus about $z = +1$,

$$\mathrm{Re}\left(\frac{1}{z^2-1}\right) = \mathrm{Re}\left(\frac{1}{z-1} - \frac{1}{z+1}\right) \approx \mathrm{Re}\left(\frac{1}{z-1}\right) = \frac{\cos\,\theta}{r}, \tag{B.17}$$

where r, θ are polar coordinates of $z-1$. The contribution to the integral Eq. B.16 from this annulus is

$$\frac{\tau_C^2}{8\pi^2 a}\int_{\zeta_1^{-1}}^{\zeta_0^{-1}}\int_0^{2\pi}\frac{\cos^2\theta}{r^2}r\,\mathrm{d}r\,\mathrm{d}\theta = \frac{\tau_C^2}{8\pi a}\ln\left(\frac{\zeta_1}{\zeta_0}\right). \tag{B.18}$$

The contribution from the annulus about $z = -1$ is the same; hence

$$E'_m(\zeta_1) - E'_m(\zeta_0) \sim \frac{\tau_C^2}{4\pi a}\ln\left(\frac{\zeta_1}{\zeta_0}\right) \tag{B.19}$$

The leading term in an expansion of $E'_m(\zeta)$ as $|\zeta| \to \infty$ is

$$E'_m(\zeta) \approx \frac{\tau_C^2}{4\pi a}\ln|\zeta|. \tag{B.20}$$

This torque-induced energy is not as large as the $O(l^2)$ force-induced energy of the previous example. Nevertheless, it is still large compared to the $O(1/l^4)$ energy associated with the curvature interaction. Under a reasonable energy relaxation process, nonzero torques on individual proteins will also undergo very rapid decay.

APPENDIX C: GEOMETRIC CONSTRAINTS ON PROTEIN CONFIGURATION

Consider those finite-energy configurations of the bilayer and proteins in which the membrane is asymptotically flat, with unit normal **3** at infinity. We will show that the balance of vertical force and horizontal torques on each protein prohibits relative vertical displacements of proteins and pivoting of any protein about any horizontal axis. Let $z = h_1(\mathbf{x})$ and $z = h_2(\mathbf{x})$ denote two configurations of the bilayer.

The finite-energy requirement is expressed by the square integrability of $\nabla^2 h_1$ and $\nabla^2 h_2$ over $\mathbf{s}$. Asymptotic flatness is expressed by ∇h_1 and $\nabla h_2 \to 0$ as $|\mathbf{x}| \to \infty$. Let $\mathbf{c}_i$ be a curve in the reference plane corresponding to the contact of the bilayer with the ith protein. We assume that the protein configuration associated with $z = h_2(\mathbf{x})$ is obtained by vertical translations and horizontal pivoting applied to the protein configuration associated with $z = h_1(\mathbf{x})$. Vertical translation does not change the curves, $\mathbf{c}_i$, and changes induced by horizontal pivoting are of second order in the pivoting angle and so are negligible in the small deflection limit considered here. Hence $\partial\mathbf{s} = \Sigma_i\mathbf{c}_i$ is the same for both configurations. The balance of vertical forces

on the *i*th protein in both configurations is given by

$$\int_{c_i} \partial_n(\nabla^2 h_i)\mathrm{d}\mathbf{s} = 0, \quad i = 1, 2. \tag{C.1}$$

The balance of horizontal torque is given by

$$\int_{c_i} [\nabla^2 h_i \hat{\mathbf{t}} - \partial_n(\nabla^2 h_i)\mathbf{J}\mathbf{x}]\mathrm{d}\mathbf{s} = 0, \quad i = 1, 2. \tag{C.2}$$

The difference between the two configurations is

$$g(\mathbf{x}) \equiv h_2(\mathbf{x}) - h_1(\mathbf{x}). \tag{C.3}$$

The square integrability of $\nabla^2 h_1$ and $\nabla^2 h_2$ implies the same for $\nabla^2 g$, and the asymptotic flatness requirements $\nabla h_1, \nabla h_2 \to 0$ as $|\mathbf{x}| \to \infty$ imply $\nabla g \to 0$ as $|\mathbf{x}| \to \infty$:

$$\int_s (\nabla^2 g)^2 \mathrm{d}\mathbf{x} < \infty, \quad \nabla g \to 0 \text{ as } |\mathbf{x}| \to \infty. \tag{C.4}$$

Because both $h_1(\mathbf{x})$ and $h_2(\mathbf{x})$ are biharmonic in $\mathbf{s}$, g must be biharmonic in $\mathbf{s}$ as well:

$$\nabla^4 g(\mathbf{x}) = 0, \quad \mathbf{x} \in \mathbf{s}. \tag{C.5}$$

Vertical translation and horizontal pivoting of proteins in configuration 2 relative to configuration 1 are expressed by the boundary conditions on g:

$$g = z_i + \mathbf{J}\mathbf{w}_i \cdot \mathbf{x}, \quad g_n = \mathbf{J}\mathbf{w}_i \cdot \hat{\mathbf{n}}, \quad i = 1, 2 \text{ on } \mathbf{c}_i. \tag{C.6}$$

Here z_i are constant vertical displacements, and $\mathbf{w}_i$ are constant 2-vectors describing the horizontal rotations. When a protein moves, its protein-bilayer contact curve and the tangent planes of the bilayer along it undergo the same rigid body movement. This determines the boundary conditions (Eq. C.6) on g and g_n along $\mathbf{c}_i$. Finally, the balances of vertical forces and horizontal torques expressed in Eqs. C.1 and C.2 lead to the following integral constraints on g:

$$\int_{c_i} \partial_n \nabla^2 g \, \mathrm{d}s = 0, \quad \int_{c_i} [\nabla^2 g \hat{\mathbf{t}} - \partial_n \nabla^2 g \mathbf{J}\mathbf{x}]\mathrm{d}s = 0. \tag{C.7}$$

In this formulation, the vertical translations z_i and rotations $\mathbf{w}_i$ are unknowns to be determined, along with g.

First we consider the consequences of $\nabla^2 g$ being square integrable and g being asymptotically flat. By the argument given in Appendix A, $\nabla^2 g$ has a multipole expansion whose leading component is quadrupole:

$$\nabla^2 g = \frac{1}{r^2}(a_2 \cos 2\theta + b_2 \sin 2\theta) + \cdots \quad \text{as } r \to \infty. \tag{C.8}$$

Corresponding solutions for g with $\nabla g \to 0$ as $r \to 0$ have the form

$$g = -\gamma \ln r + z_\infty + \frac{1}{r}(\alpha_1 \cos\theta + \beta_1 \sin\theta) + \cdots$$

$$-\frac{1}{4}(a_2 \cos 2\theta + b_2 \sin 2\theta) + \cdots \tag{C.9}$$

The first line of Eq. C.9 is the multipole expansion of a harmonic component of g, and the second line represents the component induced by the multipole expansion of $\nabla^2 g$. Note that, from the results of Eqs. C.8 and C.9,

$$g = O(\log r), \quad \nabla^2 g = O\left(\frac{1}{r^2}\right) \quad \text{as } r \to \infty. \tag{C.10}$$

Setting $h = g$ in the biharmonic Green's identity (Eq. A.2) and using the biharmonic character of g give

$$-\int_{\partial\sigma} [\nabla^2 g g_n - (\nabla^2 g)_n g]\mathrm{d}s = \int_\sigma (\nabla^2 g)^2 \mathrm{d}\mathbf{x}. \tag{C.11}$$

Here the region $\boldsymbol{\sigma}$ is taken to be the portion of $\mathbf{s}$ inside a circle $\mathbf{c}_r$ of radius r about the origin, as in Fig. 10. By virtue of the estimates (Eq. C.10), the portion of the boundary integral on the left-hand side of (Eq. C.11) corresponding to the circle $\mathbf{c}_r$ is on the order of $O((\log r)/r^2)$. Hence the $\mathbf{c}_r$ component of the boundary integral vanishes as $r \to \infty$, and the $r \to \infty$ limit of (Eq. C.11) is

$$-\sum_i \int_{c_i} [\nabla^2 g g_n - (\nabla^2 g)_n g]\mathrm{d}s = \int_s (\nabla^2 g)^2 \mathrm{d}\mathbf{x}. \tag{C.12}$$

On each boundary curve, g and g_n are given by the boundary conditions (Eq. C.6) and so becomes

$$\sum_i \left[-z_i \int_{c_i} \partial_n \nabla^2 g \, \mathrm{d}s + \mathbf{w}_i \cdot \int_{c_i} (\nabla^2 g \hat{\mathbf{t}} - (\nabla^2 g)_n \mathbf{J}\mathbf{x})\mathrm{d}s \right] = \int_s (\nabla^2 g)^2 \mathrm{d}\mathbf{x}. \tag{C.13}$$

But from the integral constraints (Eq. C.7), which impose vertical force and horizontal torque balance, it follows that the left-hand side of Eq. C.13 vanishes. Hence $\int_s (\nabla^2 g)^2 \mathrm{d}\mathbf{x} = 0$, and so g is harmonic in $\mathbf{s}$:

$$\nabla^2 g(\mathbf{x}) = 0, \mathbf{x} \in \mathbf{x}. \tag{C.14}$$

The Laplace equation (Eq. C.14) subject to boundary conditions (Eq. C.6) and asymptotic flatness at infinity constitutes an overdetermined system of equations. Below we show that g must be a uniform constant in $\mathbf{s}$. In this case, all of the rotation vectors $\mathbf{w}_i$ that appear in the boundary conditions of Eq. C.6 are zero, and all of the vertical displacements, z_i, take the same value.

Since g is harmonic, the asymptotic behavior of g as $r \to \infty$ is given by the multipole expansion in the first line of Eq. C.9. By a standard Green's identity argument, it follows that the coefficient, γ, of the log term in Eq. C.9 is given by

$$\gamma = -\frac{1}{2\pi} \sum_i \int_{c_i} g_n \, \mathrm{d}s. \tag{C.15}$$

But by the boundary condition, $g_n = \mathbf{J}\mathbf{w}_i \cdot \hat{\mathbf{n}}$ on $\mathbf{c}_i$, one has $\int_{c_i} g_n \, \mathrm{d}s = \mathbf{J}\mathbf{w} \cdot \int_{c_i} \hat{\mathbf{n}} \, \mathrm{d}s$. The line integral $\int_{c_i} \hat{\mathbf{n}} \, \mathrm{d}s$ of the unit normal around any closed curve is zero, so $\int_{c_i} g_n \, \mathrm{d}s = 0$, and it follows that γ in Eq. C.15 is zero. In this case, the dominant term in the multipole expansion (Eq. C.9) as $r \to \infty$ is the constant z_∞, and g approaches this constant asymptotically as $r \to \infty$. It follows that g achieves both maximum and minimum on the closure of the domain $\mathbf{s}$. Because g is harmonic, the maximum and minimum occur on the boundary, $\partial\mathbf{s}$. Suppose the maximum of g occurs at ∞. This maximum value is then z_∞. Because g has no log r component, the mean value of g on a large circle about the origin containing all of the $\mathbf{c}_i$ is a constant, independent of radius. The constant value must be z_∞. Because z_∞ is the maximum value of g, one must have $g \equiv z_\infty$ on all such circles, and it

follows that $g \equiv z_\infty$ in some neighborhood of ∞. But a harmonic function that is identically constant in a subregion of a connected region **s** must reduce to the same constant in the whole region **s**.

Suppose the maximum of g occurs on one of the curves $\mathbf{c}_i$. If so, the rotation vector $\mathbf{w}_i$ that occurs in the boundary conditions (Eq. C.6) must be zero. It follows from Eq. C.6 that the graph of g near $\mathbf{c}_i$ is asymptotically approximated by the plane $z = z_i + \mathbf{J}\mathbf{w}_i \cdot \mathbf{x}$, as shown in Fig. 12.

No point on $\mathbf{c}_i$ represents a maximum of g unless $\mathbf{w}_i = 0$, in which case all points on $\mathbf{c}_i$ yield the maximum value z_i of g. The boundary conditions on g along $\mathbf{c}_i$ reduce to

$$g \equiv z_i, \quad g_n \equiv 0 \quad \text{on } \mathbf{c}_i. \tag{C.16}$$

Finally, we show that the function g assumes the uniform constant value z_i in some neighborhood of $\mathbf{c}_i$. Because $\mathbf{c}_i$ is a simple closed curve, the exterior of $\mathbf{c}_i$ may be mapped conformally onto the exterior of the unit circle. Without loss of generality, $\mathbf{c}_i$ is assumed to be the unit circle in the following argument. There is an annulus $1 < r < r_m$ that does not intersect any of the other $\mathbf{c}_i$. In this annulus, g is harmonic and bounded above by z_i. Boundary conditions on $r = 1$ are $g \equiv z_i$, $g_r \equiv 0$. The mean value of g on any circle of radius r, $1 < r < r_m$, takes the form $A \ln r + B$. But the coefficient A of the log term is zero by virtue of the boundary condition $g_r = 0$ on $r = 1$. Hence the mean value of g on the circle is independent of r, and in fact must be z_i. But $z_i = \max g$, so one has $g \equiv z_i$ in the annulus $1 < r < r_m$. Therefore, g takes the uniform value z_i in some neighborhood of $\mathbf{c}_i$. Once again, we conclude that $g \equiv z_i$ in the whole connected region **s**.

APPENDIX D: BOUNDARY EFFECT ON PROTEIN ENERGETICS

The configuration of unbounded bilayer with N embedded proteins has a characteristic "tail" as $r \to \infty$. The solutions h^∞ of the Poisson equation (Eq. 12) with asymptotic flatness at spatial infinity have $r \to \infty$ behaviors given by

$$h^\infty \sim \Gamma \ln r - \frac{1}{2}(a_2 \cos 2\theta + b_2 \sin 2\theta) - \frac{1}{4r}(a_3 \cos 3\theta + b_3 \sin 3\theta) + \cdots \tag{D.1}$$

An additive constant, irrelevant to all that follows, has been omitted. The constant Γ that appears in front of the ln term arises if the proteins have nonzero contact angle γ. In fact, it is easy to show that $\Gamma = N\gamma$. The two dominant terms of this tail are an unbounded ln r component and a function with angular dependence, independent of r.

The nature of this tail raises a question about the unbounded bilayer model. A real bilayer occurs in the form of a closed vesicle, or perhaps as a patch with a clamped or pinned boundary. The tail behavior (D.1) must be modified by finite domain effects, and there is the inevitable alteration of protein energetics. There remains the question of whether the finite domain effects will be significant. If so, the protein interactions predicted by the unbounded bilayer model would never be seen in practice. We will show that the finite domain effect decreases to zero as the domain increases in size without limit.

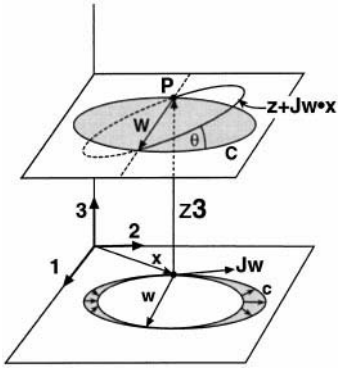

Figure 12 The graph of g near $\mathbf{c}_i$ asymptotically approximated by the plane $z = z_i + \mathbf{J}\mathbf{w}_i \cdot \mathbf{x}$, where $\mathbf{w}_i$ is the rotation vector.

We will analyze a finite domain with clamped boundary. The domain $\boldsymbol{\sigma}$ of the reference plane corresponding to the bilayer is taken to be a disk of radius $L \gg 1$ excluding disks of radius one in its interior corresponding to the proteins. Let h denote the displacement field restricted to domain $\boldsymbol{\sigma}$ with clamped boundary conditions on $r = L$, and h^∞ corresponds to an unbounded bilayer. Curves c in the reference plane corresponding to proteins are the same for clamped and unbounded configurations. A boundary value problem for the difference

$$g \equiv h - h^\infty \tag{D.2}$$

is formulated. The clamped boundary conditions on h along $r = L$ are

$$h(r = L, \theta) = H \tag{D.3}$$

$$h_r(r = L, \theta) = 0. \tag{D.4}$$

Here H is constant, and its specific value has no physical relevance, because an additive constant in h does not change the forces and energies. If H is taken to be $\Gamma \ln L$ for convenience, then from Eqs. D.1 and D.3 it is seen that the corresponding boundary values of g are

$$g(L, \theta) = \frac{1}{2}(a_2 \cos 2\theta + b_2 \sin 2\theta) + \frac{1}{4L}(a_3 \cos 3\theta + b_3 \sin 3\theta) + \cdots \tag{D.5}$$

These boundary values of g are bounded as $L \to \infty$. The boundary values of g_r that follow from Eq. D.4 are

$$g_r(L, \theta) = \frac{\Gamma}{L} + O\left(\frac{1}{L^2}\right). \tag{D.6}$$

In addition, there are boundary conditions on g along curves c representing protein-bilayer interfaces. The protein positions in the clamped bilayer are related to positions in the unbounded bilayer by vertical translations and horizontal pivoting. This restricts the admissible boundary values of g and g_r along each bilayer-protein interface c.

Recall the original derivation of force and torque balance. The variation of energy due to variations in h and h_n along c is given by $-2a\int_c[\kappa\delta h_n - \kappa_n \delta h]ds$. For an equilibrium configuration h, this boundary term is to vanish for variations δh and δh_n corresponding to vertical translation or horizontal pivoting of the protein. This is how the force and torque balances follow. Now we turn to the present problem.

The boundary values of g and g_n along c must correspond to vertical translation and horizontal pivoting of the protein. Because force and torque balance on the protein are to hold for the unbounded configuration with mean curvature $\kappa^\infty = 1/2\,(\nabla^2 h^\infty)$, and the clamped configuration with mean curvature $\kappa = 1/2(\nabla^2 h)$, there are two identities,

$$\int_c [\kappa^\infty g_n - \kappa_n^\infty g]ds = 0, \tag{D.7}$$

$$\int_c [\kappa g_n - \kappa_n g]ds = 0. \tag{D.8}$$

Subtracting Eq. D.7 from Eq. D.8, it follows that

$$\int_c [\nabla^2 g g_n - (\nabla^2 g)_n g] ds = 0. \quad (D.9)$$

Here we used $\kappa - \kappa^\infty = 1/2(\nabla^2 g)$. The information about force and torque balance is contained in any pair of the three identities Eqs. 7–9. They have immediate relevance to the following energy argument. The difference between energy densities of clamped and unbounded configurations is

$$2a(\kappa^2 - \kappa^{\infty 2}) = 2a\left[\kappa^\infty \nabla^2 g + \frac{1}{4}(\nabla^2 g)^2\right]. \quad (D.10)$$

In going from the unbounded to the clamped configuration, the energy in $\boldsymbol{\sigma}$ changes by the amount

$$\delta E_m = 2a \int_\sigma \left[\kappa^\infty \nabla^2 g + \frac{1}{4}(\nabla^2 g)^2\right] d\mathbf{x}. \quad (D.11)$$

By means of Green's identity, δE_m can be expressed as a boundary integral:

$$\delta E_m = 2a \int_{\partial\sigma} \left[\kappa^\infty g_n - \kappa_n^\infty g + \frac{1}{4}(\nabla^2 g g_n - \nabla^2 g_n g)\right] ds. \quad (D.12)$$

Here $\partial\boldsymbol{\sigma}$ consists of the large circle $r = L$ and all of the circles c of radius unity corresponding to interface with proteins. By the identities D.7 and D.9, the contribution from these circles c vanishes, leaving only a line integral on $r = L$:

$$\delta E_m = 2aL \int_0^{2\pi} \left[\kappa^\infty g_r - \kappa_r^\infty g + \frac{1}{4}(\nabla^2 g g_r - \nabla^2 g_r g)\right]\Big|_{r=L} d\theta. \quad (D.13)$$

Values of g and g_r on $r = L$ are known from Eqs. D.5 and D.6. κ^∞ and κ_r^∞ on $r = 1$ are determined from Eq. D.1. Carrying out the indicated substitutions in Eq. D.13, Eq. D.13 becomes

$$\delta E_m = \frac{2\pi a}{L^2}(a_2^2 + b_2^2) + \frac{a}{2}\int_0^{2\pi} \left[\Gamma \nabla^2 g - \frac{1}{2}(a_2 \cos 2\theta + b_2 \sin 2\theta) L \nabla^2 g_r\right]\Big|_{r=L} d\theta + O\left(\frac{1}{L^3}\right). \quad (D.14)$$

All that remains is to compute $\nabla^2 g$ and $\nabla^2 g_r$ on $r = L$, and then substitute into Eq. D.14 and carry out the integrations.

For $r = O(L)$, g may be approximated by the biharmonic field g^0 in $r < L$, which satisfies the boundary conditions D.5 and D.6:

$$g^0 = \frac{\Gamma}{2}\left[\left(\frac{r}{L}\right)^2 - 1\right] + \left[\left(\frac{r}{L}\right)^2 - \frac{1}{2}\left(\frac{r}{L}\right)^4\right](a_2 \cos 2\theta + b_2 \sin 2\theta) + O\left(\frac{1}{L}\right). \quad (D.15)$$

The "holes" in $r < L$ due to proteins are being ignored in this calculation.

Perturbations in g from g^0 due to the holes turn out to be $O(1/L^4)$, which is much smaller than the order of approximation being considered here. From Eq. D.15 it follows that

$$\nabla^2 g^0 = \frac{2\Gamma}{L^2} - \frac{6}{L^2}(a_2 \cos 2\theta + b_2 \sin 2\theta) + O\left(\frac{1}{L^3}\right) \quad (D.16)$$

$$\nabla^2 g_r^0 = -\frac{12}{L^3}(a_2 \cos 2\theta + b_2 \sin 2\theta) + O\left(\frac{1}{L^4}\right), \quad (D.17)$$

and the expression for δE_m becomes

$$\delta E_m = \frac{a}{L^2}[\Gamma^2 + 5\pi(a_2^2 + b_2^2)] + O\left(\frac{1}{L^3}\right). \quad (D.18)$$

The energy perturbation due to the clamped boundary is $O(1/L^2)$ and vanishes as $L \to \infty$.

APPENDIX E: PROOF THAT THE PENTAGONAL CONFIGURATION IS THE SMALLEST STABLE PROTEIN AGGREGATE

Recall that the interaction between a single pair is repulsive. So it remains to show that there are no $N = 3$ or $N = 4$ aggregates. Specifically, we must show that for $N = 3$ or $N = 4$, Eq. 39 cannot have solutions with all of the z_i distinct. Here we present the case $N = 4$. $N = 3$ is even easier to prove.

Given any zero energy equilibrium (z_1, z_2, z_3, z_4), one can apply any combination of translation, rotation, and dilation to the positions z_i to obtain a new equilibrium. Mathematically, such an affine transformation of the complex plane is represented by a linear transformation $z \to az + b$, where $a \neq 0$ and b are arbitrary complex numbers. The new configuration is geometrically similar to the old. By means of an affine transformation, two of the z_i, say z_1 and z_2, can be mapped into 0, 1, respectively. Hence if Eq. 39 has any solution (z_1, z_2, z_3, z_4) with z_i all distinct, it has a solution with $z_1 = 0$, $z_2 = 1$, and z_3, z_4 distinct from 0 and 1 and each other. Let us write down Eq. 39 explicitly with $z_1 = 0$, $z_2 = 1$, and z_3, z_4 as free parameters:

$$\frac{1}{1^2} + \frac{1}{z_3^2} + \frac{1}{z_4^2} = 0,$$

$$\frac{1}{1^2} + \frac{1}{(1 - z_3)^2} + \frac{1}{(1 - z_4)^2} = 0,$$

$$\frac{1}{z_3^2} + \frac{1}{(z_3 - 1)^2} + \frac{1}{(z_3 - z_4)^2} = 0, \quad (E.1)$$

$$\frac{1}{z_4^2} + \frac{1}{(z_4 - 1)^2} + \frac{1}{(z_4 - z_3)^2} = 0.$$

Adding the last two equations and using the first two in the resulting identity gives $(z_3 - z_4)^2 = 1$. Hence $z_4 - z_3 = \pm 1$, and the protein positions can be labeled so that $z_4 - z_3 = 1$. Subtracting the first two equations of Eq. E.1 from each other and setting $z_4 = z_3 + 1$ now give $(1 - z_3)^2 = (1 + z_3)^2$, so $z_3 = 0$. This is, of course, unacceptable, because $z = z_1 = 0$ is already a protein position. Hence there are no zero energy equilibria with $N = 4$ proteins.

APPENDIX F: GEOMETRIC STABILITY

The equilibrium configurations displayed in Figs. 4 and 5 are stable in the sense that they are attractors of the gradient flow differential equations (Eq. 36). But this notion of stability is physically incomplete. It is easy to see that equilibria are not isolated points $(z_1, \ldots, z_N)$ in $\mathbf{C}^N$. Given an equilibrium $(z_1, \ldots, z_N)$, any geometrically similar configuration produced by affine transformation of the complex plane is another equilibrium. So a

notion of stability should be formulated in which geometrically similar protein configurations are regarded as equivalent.

Let E be the manifold of $(z_1, \ldots, z_N)$ in $\mathbf{C}^N$ representing zero energy equilibria. A given equilibrium $(z_1, \ldots, z_N)$ is called geometrically stable if there is no path in E connecting the given equilibrium to another, geometrically dissimilar equilibrium. Otherwise, the equilibrium is called geometrically unstable. This notion of stability is the physically relevant one. Let us consider the effect of thermal fluctuations. We expect that the configuration $(z_1, \ldots, z_N)$ experiences thermal diffusion over the portion of E accessible from the initial configuration at time zero. If the initial condition is geometrically stable, there is an energy barrier to producing a geometrically dissimilar configuration. With high probability, the observed configuration over time will nearly retain geometric similarity to the initial configuration.

We formulate necessary conditions for geometric stability. Let $(z_1, \ldots, z_N)$ be an equilibrium. When written out explicitly, the equilibrium equations (Eq. 39) read

$$\eta_i = \gamma \sum_{j \neq i} \frac{1}{(z_i - z_j)^2} = 0. \tag{F.1}$$

Let z_i', $i = 1 \ldots N$ denote small perturbations of the equilibrium positions, so the new positions are $z_i + z_i'$. Corresponding perturbations of curvature scalars away from zero have linearized approximations

$$\eta_i' = 2\gamma \sum_{j \neq i} \frac{z_j' - z_i'}{(z_i - z_j)^3}. \tag{F.2}$$

If the perturbed configuration is to be an equilibrium as well, then the curvature perturbations (Eq. F.2) vanish, and the position perturbations z_i' satisfy the linear homogeneous system of equations

$$\sum_{j \neq i} \frac{z_i' - z_j'}{(z_i - z_j)^3} = 0. \tag{F.3}$$

In essence, these equations define the tangent space E' of the equilibrium manifold E at $(z_1, \ldots, z_N)$.

Two basis vectors of E' are obvious:

$$Z' \equiv (z_1', \ldots, z_N') = (1, \ldots, 1)$$
$$Z \equiv (z_1, \ldots, z_N). \tag{F.4}$$

For complex constants a, b, the linear combination $Z' = a(z_1, \ldots, z_N) + b(1, \ldots, 1) = (az_1 + b, \ldots, az_N + b)$ represents perturbations of lattice sites induced by the affine transformation $z \to (1 + a)z + b$. Hence the span of basis vectors (Eq. F.4) is called the affine subspace of E'. If the original equilibrium is geometrically stable, then the affine subspace is the whole of E'. So the question of geometric instability can be rephrased: Are there additional dimensions of E'? These would correspond to distortions of the original lattice, which breaks geometric similarity.

To find nonaffine dimensions, it is sufficient to search within a subspace of E' with two of the z_i' preset to zero, say z_i' and z_2'. Suppose there is Z' in E' outside the affine subspace. By means of an affine transformation, the positions $z_i + z_i'$ of the perturbed lattice can be mapped into a geometrically similar lattice with images of $z_1 + z_1'$ and $z_2 + z_2'$ preset to z_1 and z_2, respectively. So we get a new lattice geometrically similar to the perturbed lattice we started with, but now $z_1' = z_2' = 0$. By assumption this perturbed lattice was already geometrically dissimilar to $(z_1, \ldots, z_N)$ and remains so after the affine transformation. Hence there is Z' in E' not in the affine subspace, and $z_1' = z_2' = 0$.

A complete description of the tangent space E' by detailed analysis of the linear equations (Eq. F.3) appears formidable. But an elementary result on counting zeros of analytic functions restricts the number of zero components in any perturbation $(z_1', \ldots, z_N')$ that belongs to E'. Specifically, assume that p sites, $1 \leq p \leq N$, are perturbed and the remaining $N - p$ are not. The sites can be labeled so $z_{p+1}' = \ldots z_N = 0$, whereas the z_i, $1 \leq i \leq p$, are all nonzero. Define the meromorphic function

$$f(z) = \sum_{k=1}^{p} \frac{z_k'}{(z - z_k)^3}. \tag{F.5}$$

Requiring $\eta_i' = 0$ for $i = p + 1, \ldots, N$ amounts to requiring $f(z_i) = 0$. These requirements are, of course, necessary for

$$(z_1', \ldots, z_p', 0 \ldots 0) \tag{F.6}$$

to be in E'. Hence the nonzero perturbation with $N - p$ zero components is in E' only if $f(z)$ has at least $N - p$ zeros in $\mathbf{C}$.

Because the z_i, $1 \leq i \leq p$, are nonzero, $f(z)$ is not identically zero. In this case, the zeros of $f(z)$ are isolated, and the number of zeros inside a simple closed curve Γ of $\mathbf{C}$ is well defined. The count of zeros is carried out by a well-known formula from complex function theory. Let N_0 and N_p be the number of zeros and poles, respectively, inside Γ. The difference $N_0 - N_p$ is computed by the contour integral

$$N_0 - N_p = \frac{1}{2\pi i} \int_\Gamma \frac{f'(z)}{f(z)}\, dz. \tag{F.7}$$

The pole at z_k $(1 \leq k \leq p)$ is third order, because $z_k' \neq 0$ for $1 \leq k \leq p$. Hence $N_p = 3p$. To find the number of zeros of $f(z)$ anywhere in the complex plane, the contour Γ is enlarged in all dimensions. If $\sum_{k=1}^{p} z_k' \neq 0$, then in the large Γ limit, Eq. F.7 approaches -3, and $N_0 - N_p = -3$. If $\int_{k=1}^{p} z_k' = 0$, then the dominant behavior of $f(z)$ as $z \to \infty$ will be $O(1/z^r)$ for some integer $r > 3$. Therefore in general, $N_0 - N_p \leq -3$. Because $N_p = 3p$, the resulting bound on the number of zeros is $N_0 \leq 3p - 3$. But recall that N_0 must be greater than or equal to $N - p$ is (a very minimal) necessary condition for the perturbation Eq. F.6 to be in E', so finally $N - p \leq 3p - 3$, or

$$p \geq (N + 3)/2. \tag{F.8}$$

In summary, a nonzero perturbation $(z_1', \ldots, z_N')$ in the tangent space E' must have at least $p \geq (N + 3)/2$ nonzero components. This result has an immediate physical interpretation: an equilibrium $(z_1, \ldots, z_N)$ is stable against any perturbation that involves the displacement of fewer than $(N + 3)/2$ proteins. In Table 1, $[(N + 3)/2] \equiv$ the nearest integer $\geq (N + 3)/2$ is tabulated versus N for the first few $N \geq 5$. Recall that the smallest protein aggregate has $N = 5$. The third column tabulates $N - [(N + 3)/2]$, which represents the smallest number of proteins that can retain their initial positions under a nontrivial perturbation that preserves zero energy.

The appearance of 1 in the third column for $N = 5, 6$ is definitive in a striking way. Recall that a perturbation that breaks geometric similarity to the original lattice, if it exists, can be found within a subspace of E' with two z_i' fixed to zero. But for an $N = 5$ or $N = 6$ equilibrium, a nontrivial lattice perturbation that preserves zero energy can leave at most one lattice site unmoved. Hence there are no zero energy perturbations that break geometrical similarity with the original lattice for $N = 5, 6$. It seems that the pentagonal protein aggregate is geometrically stable. An $N = 6$ equilibrium, if it exists, would also be geometrically stable. For $N \geq 7$, the inequality F.8 by itself is not so definitive. One would have to work harder

TABLE 1

N	$\left[\frac{N+3}{2}\right]$	$N - \left[\frac{N+3}{2}\right]$
5	4	1
6	5	1
7	5	2
8	6	2
9	6	3

to show that an $N \geq 7$ lattice is geometrically stable. But this unresolved story should not distract us from the main point: at least one class of geometrically stable protein aggregates (pentagons) exists.

We thank M. Goulian, J. Keller, J. Park, and P. Pincus for critical reading of the manuscript and comments.

G. O. and K. K. were supported by NSF Grant DMS 9220719.

REFERENCES

Dan, N., P. Pincus, and S. A. Safran. 1993. Membrane-induced interactions between inclusions. *Langmuir.* 9:2768–2771.

Goulian, M., R. Bruinsma, and P. Pincus. 1993. Long-range forces in heterogeneous fluid membranes. *Europhys. Lett.* 22:145–150.

Helfrich, W. 1973. Elastic properties of lipid bilayers: theory and possible experiments. *Z. Naturforsch. C.* 28:693–703.

Landau, L. D., and E. M. Lifshitz. 1975. The Classical Theory of Fields. 4th ed. Pergamon Press, New York.

Mouritsen, O. G., and M. Bloom. 1993. Models of lipid-protein interactions in membranes. *Annu. Rev. Biophys. Biomol. Struct.* 22:145–171.

O'Neil, B. 1997. Elementary Differential Geometry, 2nd Ed. Academic Press, San Diego. xi, 482.

Park, J. M., and T. C. Lubensky. 1996. Interactions between membrane inclusions on fluctuating membranes. *J. Physique I.* 6:1217–1235.

Seifert, U., K. Berndl, and R. Lipowsky. 1991. Shape transformations of vesicles: phase diagram for spontaneous-curvature and bilayer-coupling models. *Phys. Rev. A.* 44:1182–202.

Timoshenko, S., and S. Woinowsky-Krieger. 1987. Theory of Plates and Shells. McGraw-Hill, New York.